FEA simulation of warm deep drawing process

By

Devang J Kshatriya

10MMCM11

DEPARTMENT OF MECHANICAL ENGINEERING

INSTITUTE OF TECHNOLOGY

NIRMA UNIVERSITY

AHMEDABAD-382481

MAY 2012

FEA simulation of warm deep drawing process

Major Project Report

Submitted in partial fulfillment of the requirements

For the degree of

Master of Technology in Mechanical Engineering

(Computer Integrated Manufacturing)

Prepared by

Devang J Kshatriya
(10MMCM11)

Guided by
Prof. V R Iyer

DEPARTMENT OF MECHANICAL ENGINEERING
INSTITUTE OF TECHNOLOGY
NIRMA UNIVERSITY
AHMEDABAD-382481

MAY 2012

Declaration

This is to certify that

- The thesis comprises my original work towards the degree of **Master of Technology in Mechanical Engineering (Computer Integrated Manufacturing)** at **Nirma University** and has not been submitted elsewhere for Degree.
- Due acknowledgment has been made in the text to all other material used.

Devang J Kshatriya
(10MMCM11)

Undertaking for Originality of the Work

I, **Devang J Kshatriya**, **Roll No. 10MMCM11**, give undertaking that the Major Project entitled **"FEA simulation of warm deep drawing process"** submitted by me, towards the partial fulfillment of the requirements for the degree of **Master of Technology in Mechanical Engineering (Computer Integrated Manufacturing) of Nirma University, Ahmedabad**, is the original work carried out by me and I give assurance that no attempt of plagiarism has been made. I understand that in the event of any similarity found subsequently with any published work or any dissertation work elsewhere; it will result in severe disciplinary action.

____

Signature of Student

Date:__________________

Place: NU, Ahmedabad

Endorsed by

(Signature of Guide)

Certificate

This is to certify that the Major Project Report entitled ”FEA simulation of warm deep drawing process” submitted by Mr. KSHATRIYA DEVANG J. (Roll No. 10MMCM11), towards the partial fulfillment of the requirements for the award of Degree of Master of Technology in Mechanical Engineering (Computer Integrated Manufacturing) of Nirma University of Science and Technology is the record of work carried out by him under my/our supervision and guidance. The work submitted has in my/our opinion reached a level required for being accepted for examination. The results embodied in this major project work to the best of my/our knowledge have not been submitted to any other University or Institution for award of any degree or diploma.

Prof. V R Iyee
Guide, Principal,
Institute of Diploma Studies,
Institute of Technology,
Nirma University,
Ahmedabad,

Dr. R N Patel
Head and Professor,
Department of Mechanical Engineering,
Institute of Technology
Nirma University
Ahmedabad

Dr K Kotecha
Director,
Institute of Technology,
Nirma University, Ahmedabad

Acknowledgements

It is indeed a pleasure for me to express my sincere gratitude to those who have always helped me throughout this project work.

First of all, I would like to thank my project guide Prof. V R Iyer (Principal,IDS,NU) for his consistent efforts, support, encouragement and help to achieve best possible results. I am sincerely thankful to him for his valuable guidance and interest to enhance my depth of knowledge and presentation skills.

I would like to thank Mr. T R Jain (MD, Shri Navkar Metals) and Mr. Stavan Desai (Sr. Engineer, Shri Navkar Metals). I admire them for providing me with an opportunity to work under them. In spite of having busy schedule, they were always ready to help me, whenever required. I am grateful for their patience and interest they had towards me.

Also I would like to thank my parents (Mr. J M Kshatriya, Mrs. S J Kshatriya),Rohan Kshatriya, Hetal patel,all the teachers,friends,well wishers and every one who is directly or indirectly associated with my endeavor for their support and love.

Finally special thanks to Mr.Shivraj Patil (Altair India.) for his valuable guidance for learning the software Hyper form 11.0.

Devang J Kshatriya
(10MMCM11)

Abstract

Sheet metal forming is one of the most basic and versatile process which is having highest applicability in Modern world applications , Considering wide applicability of deep drawing process in sheet metal forming product industries, this basic process has been selected for study.

Formability of sheet metal is affected by various material and process parameters, where temperature at which process is carried out plays a major role in determining the success rate and time required for manufacturing product of sheet metal.

SS 304 grade austenitic steel changes its state to martensite grade due to strain hardening during cold working process which requires annealing at definite values of strain produced in order to increase its formability,In order to eliminate this need of annealing,temperature can be combined with process by means of induction heating and control.This requires grate amount of trial and error work, Thus help of FEA SIMULATION is taken in order to predict the effect of temperature on the process variables and number of stages required to draw the component successfully thus minimizing experimental trial and error which will save time and cost of experiments.

In this study uniaxial tensile test has been performed with different specimen from all rolling direction (0,45,90 degree) at room temperature and elevated temperature in order to obtain mechanical properties of SS 304 stainless steelwhich are used as input for simulation and results are compared.In order to check effect of temperature on number of redraw required, a typical component which requires process of four stages at room temperature is chosen and attempt is made to reduce number of stages required in the process.The results show with optimum process parameters the first two stages of the four stage manufacturing process can be combined at room temperature condition,Therefore number of stages required to draw the component reduces to three stages and using elevated temperature properties first three stages of four stage manufacturing process can be combined, Therefore reducing the number

of stages required to draw the component to two using optimum parameters.

This study will help to reduce, the time required for production of typical component by reducing number of redraws required, cost of extensive experiments, and will improve productivity.

Here help of FEA simulation is taken to analyze the possibility of reduction of number of stages required from four to three at room temperature condition, and it is also shown that the process can be modified further from three stages to two stages using warm deep drawing process, which will be helpful to save the time and cost of experiment.

Contents

Declaration iii

Undertaking for Originality of the Work iv

Certificate v

Abstract vi

Acknowledgements vi

Contents vi

List of Figures xiii

List of Tables xv

Nomenclature xvi

1 Introduction 1

1.1 Metal forming . . . 1
1.2 Deep drawing . . . 2
1.3 Applications of Deep drawing process . . . 3
1.4 Parameters affecting deep drawing process . . . 3
1.4.1 Process parameters . . . 4
1.4.2 Material Parameters . . . 6
1.5 Common defects in product manufactured using deep drawing process: 8
1.6 Classification of deep drawing process depending on temperature as criteria: . . . 8
1.6.1 Cold forming . . . 8
1.6.2 Hot forming . . . 9
1.6.3 Warm forming . . . 10
1.7 Determination of force to produce required deformation in deep drawing process: . . . 10
1.8 Determination of blank size required: . . . 11

1.9 Methods for analysis of metal forming process: 12
1.9.1 Equilibrium or slab method 12
1.9.2 The slip line analysis 12
1.9.3 Upper bound technique 13
1.9.4 Viscoplasticity 13
1.9.5 Numerical methods 14
1.10 Motivation 14
1.11 Definition of problem. 15
1.12 Objective 16
1.13 Methodology 16
1.13.1 Uniaxial tensile testing at room temperature 16
1.13.2 Simulation of deep drawing process at room temperature . . . 16
1.13.3 Uniaxial tensile testing at elevated temperature 16
1.13.4 Simulation of Warm deep drawing process 17
1.13.5 Study the effect of process parameters on warm deep drawing process 17

2 Literature Survey **18**
2.1 Review of published study 18
2.1.1 Effect of temperature on anisotropy in forming simulation of aluminium alloys.[4] 18
2.1.2 Process simulation of aluminium sheet metal deep drawing at elevated temperatures.[5] 19
2.1.3 Effect of temperature on magnesium alloy component is studied and optimized using FEA and Taguchi method.[6] 19
2.1.4 Effect of temperature on plastic flow of metal and spring back is studied using FEA code Mentat and optimum temperature is selected for AMS 5604 material.[7] 20
2.1.5 Effect of temperature on LDR is studied for material AZ31 using FEA analysis.[10] 21
2.1.6 Effect of lubrication by coating chromium on die as lubricant is studied in process of warm drawing process.[8] 22
2.1.7 Effect of temperature on LDR is studied for SS 304 material using FEA analysis and suggested that simulation results matches best for temperature 120° C.[11] 23
2.2 Emperical formulas for determination of flow stress at elevated temperature 24
2.2.1 Johnson-Cook flow stress model 25
2.2.2 Steinberg-Cochran-Guinan-Lund flow stress model 25
2.2.3 Zerilli-Armstrong flow stress model 27
2.2.4 Mechanical threshold stress flow stress model 27
2.2.5 Preston-Tonks-Wallace flow stress model 29

3 Determination of mechanical properties. 31
3.1 Measurement & Dimensions of Test Specimen 31
3.1.1 Test piece preparation 31
3.1.2 Dimensions of standard test piece 32
3.2 Determination of Tensile Properties 33
3.2.1 Yield Point 33
3.2.2 Yield Strength 33
3.2.3 Reduction of Area 33
3.2.4 Tensile Strength 33
3.3 Average Tensile Properties of SS 304 tested at rolling direction of $0°, 45°$, and $90°$ 34
3.4 Chemical composition of SS 304 sheet tested 35
3.5 Determination of n,K,and r Properties 35
3.6 Evaluated properties 36

4 Simulation of four stage process at room temperature 37
4.1 FEA Simulation using Hyper Form 11.0 37
4.1.1 Pre processing 37
4.1.2 Analysis 38
4.1.3 Post processing 38
4.2 FEA Simulation of first stage 39
4.3 FEA Simulation of second stage 43
4.4 FEA Simulation of direct second stage 47
4.5 FEA Simulation of direct third stage 51

5 Determination of mechanical properties at $120°$ C temperature. 55
5.1 Measurement & Dimensions of Test Speciman 55
5.1.1 Test piece preparation 55
5.1.2 Dimensions of standard test piece 56
5.2 Average Tensile Properties of SS304 tested at rolling direction of $0°, 45°$, and $90°$ 56
5.3 Chemical composition of SS 304 sheet tested 57
5.4 Determination of n,K,and r Properties 57
5.5 Evaluated properties 59

6 Simulation of warm deep drawing. 60

7 Results and discussion 64
7.1 Uniaxial tensile testing 64
7.1.1 tensile testing at room temperature 64
7.1.2 tensile testing at $120°$ C temperature 66
7.2 Simulation results. 68
7.3 Effect of various process parameters on warm deep drawing process. . 71

8 Conclusion and Future scope **73**
8.1 Conclusion . . . 73
8.2 Future Scope . . . 74

References **75**

References **77**

Index **77**

List of Figures

1.1 Metal forming processes 2
1.2 Deep drawing Process Setup 3
1.3 four stages of production 15

2.1 Results deep drawing Process Setup 24
2.2 Result of warm deep drawing Process Setup 24

3.1 Uniaxial Tensile Test Specimen 32
3.2 Engineering True Stress-Strain Diagram 34
3.3 tensile testing machine and specimens 35

4.1 First draw product and dimensions. 39
4.2 (a)Tool setup. (b)Transparent view. 40
4.3 (a)Component of first stage draw. (b)FLD of first draw component. . 40
4.4 (a)Percentage thinning. (b)strain distributions. 41
4.5 (a)stress distribution in component. (b)Thickness distribution in component. 41
4.6 (a)Plastic strain distributions in component. (b)distribution of Von Mises stress. 42
4.7 contact force and time required 42
4.8 (a)component of second draw and (b)Dimensions of second draw component. 43
4.9 (a)Tool setup for second draw (b)transparent view. 44
4.10 (a)component after second draw. (b)FLD of second draw product. . . 44
4.11 (a)percentage thinning in second draw. (b)strain distribution. 45
4.12 (a)thickness distribution in second draw. (b)strain distribution in second draw. 45
4.13 (a)plastic strain distribution in second draw. (b)Von Mises distribution in second draw. 46
4.14 Contact forces and time required for second draw. 46
4.15 (a) Tool setup, (b) Transparent view. 47
4.16 (a) First draw component, (b) FLD of first draw component. 48
4.17 (a) Percentage of thinning, (b) strain distribution. 48
4.18 (a) stress distribution, (b) thickness distribution. 49

4.19 (a) Plastic strain distribution, (b) Von Mises distribution. 49
4.20 Contact forces between die, punch and blank with time required to draw the component. 50
4.21 (a)component, (b) dimension of component. 51
4.22 (a)Tool setup, (b) Transparent view. 52
4.23 (a)one step component, (b) FlD of one step. 52
4.24 (a)percentage thinning in component, (b) Strain distribution in component. 53
4.25 (a)percentage thinning in component, (b) Strain distribution in component. 53
4.26 (a)Plastic strain distribution in component, (b) Von Mises distribution in component. 54
4.27 Contact forces and time required. 54

5.1 Uniaxial Tensile Test Specimen 56

6.1 (a)component, (b) dimension of component. 60
6.2 (a)Tool setup, (b) Transparent view. 61
6.3 (a)first draw component, (b) FLD using temperature for first draw. . 61
6.4 (a)percentage thinning, (b) strain distribution. 62
6.5 (a)Stress distribution, (b) Thickness distribution. 62
6.6 (a)Plastic strain distribution, (b) Von Mises distribution. 63
6.7 contact forces and time required. 63

7.1 True stress Vs True Strain diagram for 0° sample 64
7.2 True stress Vs True Strain diagram for 45° sample 65
7.3 True stress Vs True Strain diagram for 90° sample 65
7.4 True stress Vs True Strain diagram for 0° sample 66
7.5 True stress Vs True Strain diagram for 45° sample 66
7.6 True stress Vs True Strain diagram for 90° sample 67
7.7 True stress Vs True Strain diagram for 90° sample 72
7.8 True stress Vs True Strain diagram for 90° sample 72

List of Tables

3.1 Dimensions of Standard Specimens 32
3.2 Tensile Properties of Tested SS304 34
3.3 Chemical Properties of Tested SS304 35
3.4 Evaluated Properties 36

4.1 Parameters used for simulation 39
4.2 Parameters used for simulation of second stage 43
4.3 Parameters used for simulation direct second stage 47
4.4 Parameters used for simulation direct third stage 51

5.1 Dimensions of Standard Specimens 57
5.2 Tensile Properties of Tested SS304 57
5.3 Chemical Properties of Tested SS304 58
5.4 Evaluated Properties 59

6.1 Properties used for warm simulation of direct third stage 60

7.1 Comparison of mechanical properties 67
7.2 Results from simulation of first stage at room temperature 68
7.3 Results from simulation of second stage at room temperature 68
7.4 Results from simulation of direct second stage at room temperature . 69
7.5 Results from simulation of direct third stage at room temperature . . 70
7.6 Results from simulation of direct third stage product with 120°C temperature 71

Nomenclature

σ_{tau} : True Stress (N/mm^2) 3.3
e : Engineering Strain 3.3
σ_E : Engineering Stress 3.3
ϵ : True Strain 3.3
n : Strain Hardening Exponent 3.3
K : Strength Co-efficient 3.3
x : ln(True Stress) 3.3
y : ln(True Strain) 3.3
N : No. of Data Points 3.3
r_0 : Longitudinal Anisotropy 3.3
r_{45} : Diagonal Anisotropy 3.3
r_{90} : Traverse Anisotropy 3.3
r : Anisotropy Index 3.3
δw : Change in width(mm) 3.3
w_0 : Original Width(mm) 3.3
δt : Change in Thickness(mm) 3.3
t_0 : Original Thickness(mm) 3.3

Chapter 1

Introduction

1.1 Metal forming

Forming is a broad term covering many different manufacturing processes. In general, you may think of forming as any process that changes the shape of a given raw stock without changing its phase (i.e. without melting it). In general, these processes involve beating with a hammer, squeezing, bending, pulling/pushing through a hole, etc.

Practically all metals, which are not used in cast form, are reduced to some standard shapes for subsequent processing. Manufacturing companies producing metals supply metals in form of ingots which are obtained by casting liquid metal into a square cross section.

- Slab (500-1800 mm wide and 50-300 mm thick)
- Billets (40 to 150 sq mm)
- Blooms (150 to 400 sq mm)

Sometimes continuous casting methods are also used to cast the liquid metal into slabs, billets or blooms. These shapes are further processed through hot rolling, forging or extrusion, to produce materials in standard form such as plates, sheets, rods, tubes and structural sections.[3]

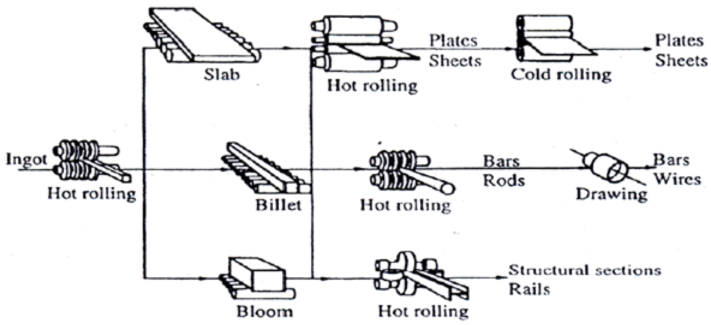

Figure 1.1: Metal forming processes

Primary metal forming processes:

- Rolling
- Forging
- Extrusion
- Tube and wire drawing
- Spinning
- Deep drawing

1.2 Deep drawing

The term deep drawing implies that some drawing - in of the flange metal occurs and that the formed parts are deeper then could be obtained by simply stretching the metal over die.[1]

Flat sheet metal is formed into cylindrical or box type parts by means of punch that presses blank into die cavity, thus the component formed is the result of combined controlled moment of punch and flow of material in the die, and here important value is the L/D ratio of the component.

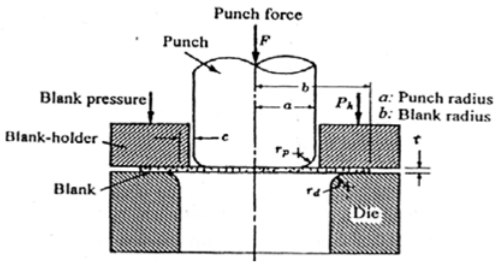

Figure 1.2: Deep drawing Process Setup

1.3 Applications of Deep drawing process

It is one of the most important manufacturing processes especially with those components which cannot have desired physical and mechanical properties if produced by casting process, Practically all metals, which are not used in cast form, can be easily produced by deep drawing process.

Applications of deep drawing:

- Kitchen wares
- Boxes of various shapes
- Components of car bodies
- Domestic gas cylinder
- Milk cans
- Defence equipment parts

1.4 Parameters affecting deep drawing process

Process of deep drawing is governed by two types of major parameters (1) Process parameters and (2) Material parameters

1.4.1 Process parameters

- **Blank holding force**

Blank holding is required in order to avoid wrinkling by keeping sheet flat and to prevent its buckling under the action of induced circumferential compression, thus blank holding at end of blank is necessary to avoid wrinkles and also to facilitate flow of metal at die profile radius.

Value of blank holding force should be optimum as too large force will increase frictional stresses in flange drawing which ultimately results in higher stresses in cup wall and at the punch profile radius where due to bending under tension the thinning and necking may take place, in fact as the punch proceeds blank holding force required for the process decreases, lower values then required will produce wrinkles on the cup, thus value of blank holding force should be optimum which is given by,

$$F_h = A_c \times p_a$$

Where,

A_c = area of contact between die, blank and blank holder

$$= \left(\frac{\pi}{4}\right)\left[D^2 - (d_p + 2 \times r_{cd})^2\right]$$

And p_a= Average blank holding pressure (empirical formula)

$$= \left[\left(\left(\frac{D}{d_p}\right) - 1\right)^3 + 0.005\left(\frac{D}{t}\right)\right]\sigma_u$$

Where,

d_p = dia of punch.

r_{cd} = Die profile radius.

D = Blank diameter

K = constant depends on thickness of blank and type of material

t = thickness of sheet.
σ_u = ultimate tensile strength of blank material.
Some other empirical relations are,

$$p_a = \left[\left(\left(\frac{D}{d_p} \right) - 1 \right)^3 + \left(\frac{1}{t^{\frac{1}{8}}} \right) \right] \sigma_u$$

- **Co-efficient of friction or lubrication**[2]

Lubrication between die and blank reduces the co-efficient of friction thus drawing stresses are low, but rough and dry punch blank interface will increase friction on punch profile radius will restrain the neck formation and will give higher drawability.

- **Clearance between punch and die**

Radial clearance between punch and die controls the freedom of cup walls either to thicken or to taper and pucker, Clearance between punch and die affects the ironing effect on cup, in deep drawing process clearance value is generally between 0.1 to 0.3 times thickness of sheet metal depending on type of drawing and reduction , it accounts for friction and bending.

- **Die and punch profile radius**

Die radius affects the maximum punch load required to draw as sharp radius increases process work due to plastic bending under tension, higher values of die radius lowers the limiting draw ratio, thus generally die radius value is taken as 10 times of blank thickness.
Punch profile radius is most important as fracture usually occurs around punch profile, generous the punch profile radius is more gradual is the rise of punch load as the punch travels, but the maximum punch load is almost unaffected.

- **Drawing speed**

It affects the yield stress of the material as it affects the strain rate sensitivity of the material, but with good lubrication the effect of punch speed can be reduced.

- **Temperature**

$$\sigma_f = K\left(\varepsilon^{\circ}\right)^{\eta}$$

Temperature affects the flow stress of material directly , which is nothing but the stress value require to maintain plastic deformation, with increase in temperature strain rate sensitivity of material increases but it reduces the strength co-efficient k of metal thus flow stress reduces.

1.4.2 Material Parameters

- **Average Anisotropy**

The r value, or plastic strain ratio, relates to drawability and is known as the anisotropy factor. This is defined as the ratio of the true width strain to the true thickness strain in the uniform elongation region of a tension test.

$$r = \frac{\ln\left(\triangle w / w_0\right)}{\ln\left(\triangle t / t_0\right)}$$

The r value is a measure of the ability of a material to resist thinning. In drawing, material in the flange is stretched in one direction (radially) and compressed in the perpendicular direction (circumferentially). A high r value indicates a material with good drawing properties. The r value frequently changes with direction in the sheet. In a cylindrical cup drawing operation, this variation leads to a cup with a wall that varies in height, a phenomenon known as earing. It is therefore common to measure the average r value, or average normal anisotropy, r_m, and the planar anisotropy δr.

- **Strain hardening exponent η**

$$\sigma_T = K\varepsilon^{\eta}$$

η is determined by the dependence of the flow (yield) stress on the level of strain. In materials with a high n value, the flow stress increases rapidly with strain. high ? value is also an indication of good formability in a stretching operation, in the region of uniform elongation.

- **LDR**

It is the ratio of maximum blank diameter that can be drawn / inside diameter of cup, the punch load increases with increase in blank diameter in approximately linear manner with a slight tendency to drop near limiting draw ratio. If this ratio above 2 to 2.4 then generally redrawing is carried out, thus in redrawing diameter of cup is reduced and length of cup is increased and also thickness of cup is also reduced, stages of redrawing required can be reduced by using material with higher values of η.

- **Yield strength and pre straining.**

- **Young's modules, Poisson's ratio, strength co-efficient, ultimate stress, spring back, etc.**

These are the parameter that mainly affects the stress produced in the cup during the process and hence ultimately affect the drawing force required and time required for completing the process.

- **Percentage reduction or thinning allowed**

Percentage reduction = 100 (1 - d / D)
It usually depends on the blank sheet diameter and of cup required in final component, percentage reduction also affects number of redraws required to produce component.

- **Grain size and hardness of sheet metal.**

Grain size affects the atomic dislocation within material, thus material with courser grain size will fail at much lower values of stress then with finer grain size.

Hardness of blank material also affect the process as with increases in hardness drawability decreases, but with low hardness the strength of cup will be affected, thus hardness of material must be adequate.

1.5 Common defects in product manufactured using deep drawing process:

(1) Earing

(2) Wrinkles

(3) Stretch marks in cup wall, etc.

1.6 Classification of deep drawing process depending on temperature as criteria:

These are on the basis of working temperature in reference of recrystallization temperature.[?]

1.6.1 Cold forming

It is the plastic deformation of metals and alloys below recrystallization temperature and strain rates are such that strain hardening is not relived, generally it is carried out at room temperature, cold working increases strength and hardness but decreases the ductility of metal, thus if the metal is excessively deformed it may fracture before it is formed, large deformation in cold working requires intermediate annealing.

Characteristics of cold working:

(A) Forces required for deformation are higher.

(B) Strain hardening increases strength of material thus inferior metals can be used.

(C) Excellent surface finish

(D) High dimensional accuracy

(E) No oxidation and scaling can give tighter tolerances

(F) Lubrication is easier

Disadvantages:

(A) Limited formability

(B) Flow stresses are higher requiring higher forces for deformation hence higher power

(C) Due to strain hardening stress relieving is required

1.6.2 Hot forming

It is working of preheated material above recrystallization such that recovery and recrystallization takes place simultaneously with deformation, hot working occurs at constant flow stress.

Characteristics of hot working:

(A) Low flow stress and high ductility requires less drawing force and power

(B) Good formability

(C) Large deformation is possible in single stage

(D) Blow holes and porosity are automatically eliminated

(E) Does not require stress relieving

Disadvantages:

(A) Additional energy is required to heat material

(B) Metal oxides and scale impair surface finish

(C) Due to surface carburization surface strength and hardness of steel component reduces.

(D) Thin gauge sheets cannot be made

1.6.3 Warm forming

Here the temperature is above room temperature but below recrystallization temperature, generally between 0.3Tm to 0.5Tm thus advantages of both hot and cold forming is combined.
Temperature range is low to avoid scaling thus producing good surface finish, increasing temperature increase strain rate sensitivity but reduces strength coefficient yet they are high enough to reduce flow stresses provided strain rates are kept low.

1.7 Determination of force to produce required deformation in deep drawing process:

Drawing force required to produce plastic deformation depends on the stress produced in the blank at different section of the die which is the combination of
(1) Compressive circumferential stress
(2) Tensile radial stress
(3) Compressive blank holding force

Where blank is subjected to stresses due to following different forces produced as punch advances in the die.

(1) Bending over punch profile radius
(2) Drawing of flange under friction between die and blank holder
(3) Bending of sheet at die profile radius
(4) Slipping of sheet over die profile radius
(5) Unbending of sheet into cup wall

Drawing force (Empirical formula):

$$F = \pi d t \sigma_0 \left(D/d - c\right)$$

Where,

d = outer diameter of cup, mm.

D= blank diameter, mm.

t = blank thickness, mm.

σ_0 = tensile yield strength of metal, MPa.

c = constant for accounting for friction and bending, (0.6 to 0.7)

Drawing force (Theoretical formula):

$$F \approx 2\pi r_p t \sigma_z$$

Where,

r_p = radius of punch, mm

σ_z = stress in thickness direction, N/mm2.[3]

1.8 Determination of blank size required:

Diameter of blank required to produce component is given by following formula,

$$D = \left(d^2 + 4dh\right)^{0.5} \qquad When\ d \geq 20r_{cp}$$

$$D = \left(d^2 + 4dh - 0.5r_{cp}\right)^{0.5} \qquad When\ 15r_{cp} \leq d \leq 20r_{cp}$$

$$D = \left(d^2 + 4dh - r_{cp}\right)^{0.5} \qquad When\ 10r_{cp} \leq d \leq 15r_{cp}$$

$$D = \left[(d - 2r_{cp})^2 + 4d\left(h - r_{cp}\right) + 2\pi r_{cp}\left(d - 0.7r_{cp}\right)\right]^{0.5} \qquad When\ d < 10r_{cp}$$

Where,

r_{cp} = Punch profile radius

d = outer diameter of cup

h = height of shell

For redrawing operation l/d ratio can be calculate as

$$l/d_n = (1/4)\left[\left(\frac{D}{d_0}\right)^2 - 1\right]$$

Where d_n = diameter of cup after n^{th} draw

1.9 Methods for analysis of metal forming process:

1.9.1 Equilibrium or slab method

Representative element from the body of material undergoing plastic deformation and identifying normal and frictional forces acting on this element, behavior of element is analyzed by considering equilibrium of forces acting on it at any instant of deformation.

This method approximates and underestimates the magnitude of forces involved by virtue ironing, particularly suitable for wire and tube drawing, hot and cold rolling of strips and sheets, rotary piercing, and elongation of tubing. By introducing stress redundancy factor or by modifying the value of yield stress in integration of equilibrium we can obtain more accurate results.

1.9.2 The slip line analysis

Generally applied to plain strain conditions, deforming body is assumed to be rigid, perfectly plastic, and isotropic, here a family of straight or curvilinear lines (slip line field) is formed which intersect with each other orthogonally, corresponds to direction of yield stress of material in shear, network of lines must satisfy the condition of static equilibrium of forces, yield criterion, boundary conditions, and they must be compatible with velocity field to maintain mass continuity.

This method is used successfully in the analysis of forging, rolling and extrusion to predict stresses, loads, direction of material flow, and temperature variations within the material.
Most serious limitation is that accuracy of results depends on the condition of plain strain, thus cannot be satisfactorily used for majority of antisymmetric problem.

1.9.3 Upper bound technique

Overall deformation zone is divided into number of smaller zones with in which velocity of arrival is continuous, here moment of all the zones and boundaries should be such that discontinuity in velocity occur only in tangential direction,
Total power consumed in operation P = P_1 +P_2 +P_3
Where,
P_1 = ideal power of deformation
P_2 = power consumed in shearing of material in direction of velocity discontinuity
P_3 = power required in overcoming friction at die work piece interface.

Finally velocity field that minimizes the total calculated power is taken as actual one and is compared with experimental data, this method over estimates the load and is applicable in metal working operations.

1.9.4 Viscoplasticity

Experimental technique to determine strain rates and stress distribution in the deformation zone, here grid pattern is placed on flat surface and observing the distortion of grid after subjecting to an infinitesimal incremental deformation, the process is repeated number of times.
From the distortions, the strain rates are calculated and then using plasticity equations stresses are calculated, technique can be used for plain strain and axisymmetric cases, accuracy depends on the accuracy of placement of rigid grid and measurement

after each incremental deformation, redundancy can be eliminated at the stage of examination of grid distortion.

1.9.5 Numerical methods

- **Finite element method**

Deformation zone in an elastic body is divided into number of elements interconnected at finite number of nodal points, then actual velocity distribution is estimated for each element, simultaneous equations are developed representing unknown velocity vectors, thus from solutions actual velocity distributions and stresses are calculated.

- **Finite difference method**

Technique can incorporate friction conditions at die work piece interface and actual properties of material, applied in bulk deformation like sheet metal forming problems; it gives detailed outline of stresses, strain distribution throughout the work piece.

1.10 Motivation

- SS 304 is Austenitic steel which changes its phase to martensite due to strain hardening, making annealing compulsory if grater deformation is required without failure.force required to produce the deformation increases with increase in strain, requirement of annealing also increases all over production time of the component.

- Warm forming process can be employed to address such problems.

- FEM analysis can help to reduce time required for trial and experiments, it also helps to find combination of optimum parameters to achieve successful forming of component by predicting any defect during early stages hence cost and time of defective production and tryouts can be saved. The production of high quality formed products in a short time and at a low cost is an ultimate goal in manufacturing which can be achieved by using FEM.

1.11 Definition of problem.

From the literature published it was seen clearly that temperature affects the process of deep drawing up to a great extent for both ferrous as well as non ferrous metals, it is also found that for SS 304 grade metal how LDR ratio increases by 24% by incorporating temperature of 120°, and results of simulation matches with experimental results by the error of just 2.3%, hence temperature of 120° is selected.

A typical component is selected which requires manufacturing process of four stages, from material SS 304, as shown in figure below.

Figure 1.3: four stages of production

The idea was to reduce or eliminate the number of stages required to produce the component in order to increase the production and optimize the process parameters using FEA in order to save the time required and cost of experimenting.

1.12 Objective

Primary objective of "FEA simulation of warm deep drawing process" is to simulate the process of warm deep drawing using FEA to check effect of temperature on deep drawing process such that number of stages required to produce a typical component can be reduced or eliminated.
Secondary objective is to study the effect of various process parameters on deep drawing process.

1.13 Methodology

1.13.1 Uniaxial tensile testing at room temperature

Material properties like yield strength,co-efficient of strength, strain hardening exponent(n), anisotropy(r) for all three rolling directions,are obtained at room temperature for SS 304 metal sheet having thickness 1.17 mm using FIE make Universal testing machine,UTES-40 and yield is calculated by 5% strain offset as per ASTM E8.

1.13.2 Simulation of deep drawing process at room temperature

Simulation of four stage manufacturing process of component is done using room temperature properties by FEA tool Hyper Form 11.0 to check the results of simulation. suggestion have been made to combine first two stages of the original four step process, and results have been validated for combination of first two stages.

1.13.3 Uniaxial tensile testing at elevated temperature

Material properties such as Yield strength, co-efficient of strength,strain hardening exponent(n),anisotropy for all three rolling direction, are obtained at 120 degree centigrade for same metal SS 304 sheet having thickness 1.17 mm according to standard

ASTM E-21:2009 yield is calculated at 5% strain offset.

1.13.4 Simulation of Warm deep drawing process

Using mechanical properties obtained at elevated temperature FEA Simulation of warm deep drawing process is done in order to combine first two stages of modified three stage process using optimum parameters.

1.13.5 Study the effect of process parameters on warm deep drawing process

Effect of various process parameters like different punch velocity and blank holding force,on deep drawing process is done and results are discussed.

Chapter 2

Literature Survey

2.1 Review of published study

2.1.1 Effect of temperature on anisotropy in forming simulation of aluminium alloys.[4]

• S. Kurukuri, A. Miroux, M. Ghosh.

A combined experimental and numerical study of the effect of temperature on anisotropy in warm forming of AA 6016-T4 aluminum was performed. From the presented warm forming simulations of the cylindrical cup deep drawing, it is seen that the effect of temperature on shape change of yield locus has an effect notably on the predicted thickness distribution, indeed the predicted thickness with the model including temperature effects is almost overlaps the experimentally measured thickness at the bottom. In the die radius area also, the model with temperature effects performs slightly better than the one obtained without temperature effects. However the model cannot represent the experimental earing profile at elevated temperatures.

2.1.2 Process simulation of aluminium sheet metal deep drawing at elevated temperatures.[5]

• Johannes Winklhofer, Gernot Trattnig, Christoph Lind.

disadvantage of aluminium is that it is less formable than steel, Therefore complex part geometries can only be realized by expensive multi-step production processes. One method for overcoming this disadvantage is deep drawing at elevated temperatures. the formability of aluminium sheet metal can be improved significantly, and the number of necessary production steps can thereby be reduced.

The temperature and strain rate dependent material properties of a 5xxx series alloy and their modeling are discussed, LS-Dyna can be used conveniently for the simulation of aluminium sheet metal deep drawing processes at elevated temperatures, although there is still the lack of a temperature dependent anisotropic material model.Process parameters and their dependence on temperature, in particular the friction coefficients, have to be investigated and described for the process simulation of warm forming of aluminium sheet metal. Increasing the tool velocity in warm forming of aluminium sheet metal is practical for industrial application, but has a negative influence on formability. Tailor made tooling for warm forming of complex geometries is a future field of research and engineering.

2.1.3 Effect of temperature on magnesium alloy component is studied and optimized using FEA and Taguchi method.[6]

• Hong seok kim, Muammer Koc, Jun Ni.

Taguchi method along with FEM method solver ABAQUS is used to determine temperature distribution zone in magnesium alloy A5083p is carried out, heaters and coolers for process are not designed in to simulation model instead uniform temperature condition is directly assigned to the material model, here change in temperature by conduction and convection are taken into account on part of blank holder, blank

holding force is kept constant, entire model is described by thermally coupled 4 node bilinear element CAX4RT, punch speed is also kept constant.
Both cold deep drawing and warm deep drawing were simulated where cold deep drawing shown 30% thinning around punch corner radius at a depth of 13 mm where as in case of warm deep drawing same thinning is observed at depth of 33 mm thus higher drawability is achieved by warm deep drawing process simulation
Comparison of LDR at different punch speed and temperature are plotted and it is observed that the error in simulation of warm deep drawing is too small making results accurate and valid.Taguchi method id used to obtain proper temperature zone to get maximum formability, response graphs were plotted and thus recommended temperature for punch 25C, blank 25C, blank holder 250C, and die 180C are recommended'

2.1.4 Effect of temperature on plastic flow of metal and spring back is studied using FEA code Mentat and optimum temperature is selected for AMS 5604 material.[7]

• F. STACHOWICZ, T. TRZEPIECISKI.
The aim of warm sheet metal forming processes is to improve plastic flow of material, as well as to decrease the spring back effect. with the effect of temperature in the range from 20C to 700C on basic material parameters of stainless steel sheet metal such as yield stress, ultimate strength, total and uniform elongation, strain hardening parameters and plastic anisotropy factor. It was determined that the most suitable temperature of warm forming of the AMS 5604 stainless steel sheet is 500C. The MSC Marc Mentat commercial computer code was used for numerical simulation of analyzed forming processes.
Examination on spring back quantity was performed in air bending test.optimal temperature for a particular warm forming operation and formed material lower limit is determined by force which can be produced by the forming machines and by the

formability of the material. The upper limit is usually determined by the amount of oxidation which can be tolerated. satisfactory lubricant which has to meet the lubrication criteria graphite-based lubricants have proved particularly suitable and are normally applied onto the tool surface since graphite oxides above 770 K. The investigations, suggested the possibility of drawing stainless steel for structural parts at moderate elevated temperature rather than drawing them in the annealed state and heat treating after forming, chemical composition of AMS 5604 stainless steel sheet is Cr 16.5, Ni 4.0, Cu 4.0, Mn 1.0, Mo 0.5, Si 1.0, Nb 0.3, C 0.07 wt.%., Uniaxial tensile test was performed to determine mechanical parameters of the 1.0 mm thick stainless steel at different temperature range. The strain-stress relation was described employing Hollomon equation in the form of:

$$\sigma = K\varepsilon^{\eta}$$

, sheet metal induction heating, sheet metal induction heating and forming die flame heating, electric heating in isothermal conditions.
Marc Mentat commercial computer code can predict the spring back effect with very high accuracy and hence can be used for metal working simulation.

2.1.5 Effect of temperature on LDR is studied for material AZ31 using FEA analysis.[10]

• G. Palumbo, D. Sorgente, L. Tricarico,S.H. Zhang,W.T. Zheng.
An improvement of the Limit Drawing Ratio from 1.8 up to 2.6 is feasible when adopting a Draw Die temperature equal to 170C. equipment was designed to perform WDD tests superimposing different thermal gradient by (i) heating the blank holder and/or the female die; (ii) cooling the punch using a water flow. The FE approach allowed reducing the experimental tests to be performed. In particular 2D fully coupled thermo-mechanical model of the WDD process was created experimental activities were combined with numerical simulations using ABAQUS the Finite

Element (FE) technique which is nowadays largely diffused as optimization tool WDD tests on circular blanks in AZ31 with thickness 0.6mm were Performed.
Finite Element (FE) model was used for investigating the more efficient positioning of the electric heaters (into the Blank Holder or into the Draw Die); the prediction of critical conditions occurrence was based on the qualitative comparison with the AZ31 Forming Limit Diagram from literature.
The experimental procedure in the WDD tests is followed: (1) to heat the female die and the blank holder up to the test temperature, being the punch and the blank at room temperature; (2) to assemble the blank; (3) waiting few minutes for heating the blank up to the temperature of the female die; (4) to move down the punch to deform the blank.
WDD tests aimed to form cylindrical cups were performed using a constant punch speed 10mm/min and different temperature levels120C, 140C, 150C, 160C, 170C,Punch Load; in particular when comparing the maximum DD force concerning the CP and the CPC heating conditions, considering the very similar temperature levels in the blank center region, a large difference was recognized, which could be due to temperature difference realized in the Blank Holder. CPC heating technique.

2.1.6 Effect of lubrication by coating chromium on die as lubricant is studied in process of warm drawing process.[8]

• Jae Dong Lee, Young Moo Heo, Sung Ho Chang.
The die was coated with chromium coated for the purpose of lubrication in warm deep drawing process for material of EDD steel, the effect of lubrication on limiting drawing ratios, maximum drawing force and maximum drawing depth are studied and also thickness strain distribution is studied, the temperature range is between room temperature90o to 250oC., drawing ratios ranging from 2.4 to 2.9 are considered, UTM is used to determine the material properties at elevated temperatures, analysis using an FEM code (DYNA-3D).

The LDR increases as the temperature increases. The numerical blank model was divided into a cooling zone and a heating zone. The temperature of the heating zone was gradually increased and, during the computation, temperature-dependent material properties were used. The numbers of elements and nodes are 4225 and 4429, respectively.

The limiting drawing ratio and the maximum drawing depth increase and the maximum drawing force decreases as the die temperature increases. The distribution of through-thickness, strain is more uniform at elevated temperatures than that at room temperature, and the difference between the maximum and minimum through -thickness strains decreases. Numerical simulation using an FEM code, the distribution of through-thickness strain generally agreed with the experimental results. But, a big discrepancy at the head of the punch was observed, the effect of heat transfer between the punch and blank should be considered to obtain more accurate results.

2.1.7 Effect of temperature on LDR is studied for SS 304 material using FEA analysis and suggested that simulation results matches best for temperature 120° C.[11]

- Takuda ,K. Mori, T. Masachika ,E. Yamazaki , Y. Watanabe.

The forming limit in warm deep drawing of a type 304 stainless steel sheet is experimentally examined and the deformation behavior and the temperature change in the sheet are simulated by the combination of the rigid-plastic and the heat conduction finite element methods considering deformation-induced martensitic transformation for type 304 stainless steel.

Effect of temperature on different LDR, drawing force, and drawing depth are simulated using FEM method at different elevated temperatures,It is seen that for the same blank diameter at temperature of 120oC LDR increases from 2.1 to 2.7, with change in thickness less than 10 Thus the limiting DR becomes remarkably higher in the warm deep drawing than that at room temperature. Such improvements can be

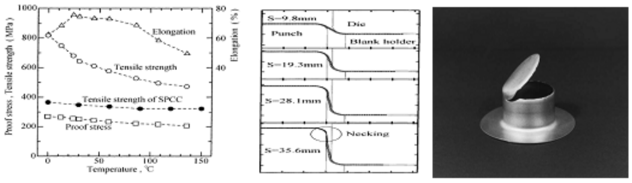

Figure 2.1: Results deep drawing Process Setup

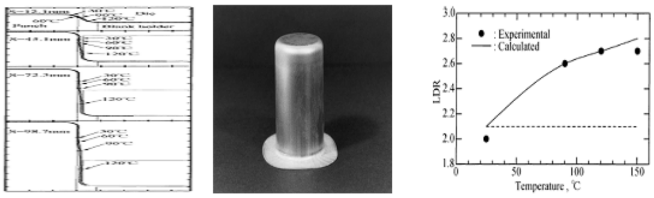

Figure 2.2: Result of warm deep drawing Process Setup

attained by the comparatively low heating temperature under for the stainless steel sheet. The forming limit and the fracture initiation site can be successfully predicted by the finite element methods.

2.2 Emperical formulas for determination of flow stress at elevated temperature

Numerous empirical and semi-empirical flow stress models are used the computational plasticity. The following temperature and strain-rate dependent models provide a sampling of the models in current use:

1. Johnson-Cook model
2. Steinberg-Cochran-Guinan-Lund model.
3. Zerilli-Armstrong model.
4. Mechanical Threshold Stress model.
5. Preston-Tonks-Wallace model. .

2.2.1 Johnson-Cook flow stress model

The Johnson-Cook (JC) model is purely empirical and is the most widely used of the five. However, this model exhibits unrealistically small strain-rate dependence at high temperatures.gives the following relation for the flow stress (σ_y).

$$\sigma_y\left(\varepsilon_p, \overset{\circ}{\varepsilon}_p, T\right) = [A + B(\varepsilon_p)^n] + \left[1 + C\ln\left(\varepsilon^{\circ *}_{p}\right)\right]\ [1 - (T^*)^m]$$

where ε_p is the equivalent plastic strain, $\varepsilon^{\circ}{}_p$ is the plastic strain-rate, and A,B,C,n,m are material constants.

The normalized strain-rate and temperature in equation (1) are defined

$$\varepsilon^{\circ *}_{p} = \frac{\overset{\circ}{\varepsilon}_p}{\overset{\circ}{\varepsilon}_{p0}} \qquad and \quad T^* = \frac{(T - T_0)}{(T_m - T_0)}$$

where $\overset{\circ}{\varepsilon}_{p0}$ is the effective plastic strain-rate of the quasi-static test used to determine the yield and hardening parameters A,B and n. This is not as it is often thought just a parameter to make $\varepsilon^{\circ *}_{p}$ non-dimensional. T_0 is a reference temperature, and T_m is a reference melt temperature. For conditions where $T^* < 0$, we assume that m = 1.

2.2.2 Steinberg-Cochran-Guinan-Lund flow stress model

The Steinberg-Cochran-Guinan-Lund (SCGL) model is semi-empirical. The model is purely empirical and strain-rate independent at high strain-rates and extended to low strain-rates and bcc materials by Steinberg and Lund for high strain-rate situations. A dislocation-based extension based on is used at low strain-rates. The SCGL model is used extensively by the shock physics community.

The Steinberg-Cochran-Guinan-Lund (SCGL) model is a semi-empirical model that was developed by Steinberg et al.for high strain-rate situations

$$\sigma_y\left(\varepsilon_p, \overset{\circ}{\varepsilon}_p, T\right) = \left[\sigma_a f\left(\varepsilon_p\right) + \sigma_t\left(\overset{\circ}{\sigma}_p\right)\right] \frac{\mu\left(p, T\right)}{\mu_0} \qquad \sigma_a \le \sigma_{max}\ and\ \sigma_t \le \sigma_p$$

where σ_a is the thermal component of the flow stress, $f(\varepsilon_p)$ is a function that represents strain hardening, σ_t is the thermally activated component of the flow stress, $\mu(p,T)$ is the pressure and temperature-dependent shear modulus, and μ_0 is the shear modulus at standard temperature and pressure. The saturation value of the thermal stress is σ_{max}. The saturation of the thermally activated stress is the Peierls stress σ_p. The shear modulus for this model is usually computed with the Steinberg-Cochran-Guinan shear modulus model.

The strain hardening function (f) has the form

$$f\left(\varepsilon_p\right) = \left[1 + \beta\left(\varepsilon_p + \varepsilon_p i\right)\right]^n$$

where β, n are work hardening parameters, and $\varepsilon_p i$ is the initial equivalent plastic strain.

The thermal component (σ_t) is computed using a bisection algorithm from the following equations.

$$\overset{\circ}{\varepsilon}_p = \left[\frac{1}{c_1} exp\left[\frac{2U_k}{k_b T}\left(1 - \frac{\sigma_t}{\sigma_p}\right)^2 + \frac{C_2}{\sigma_t}\right]\right]^{-1} ; \qquad \sigma_t \leq \sigma_p$$

where $2U_k$ is the energy to form a kink-pair in a dislocation segment of length L_d, k_b is the Boltzmann constant, σ_p is the Peierls stress. The constants C_1, C_2 are given by the relations

$$c_1 = \frac{\rho_d L_d a b^2 v}{2w^2} \qquad c_2 = \frac{D}{\rho_d b^2}$$

where ρ_d is the dislocation density, L_d is the length of a dislocation segment, a is the distance between Peierls valleys, b is the magnitude of the Burgers vector, v is the Debye frequency, w is the width of a kink loop, and D is the drag coefficient.

2.2.3 Zerilli-Armstrong flow stress model

The Zerilli-Armstrong (ZA) model is based on simplified dislocation mechanics. Model is a simple physically based model that has been used extensively. The general form of the equation for the flow stress is

$$\sigma_y\left(\varepsilon_p, \overset{\circ}{\varepsilon}_p, T\right) = +B\ exp\left(-\beta\left(\overset{\circ}{\varepsilon}_p\right)T\right) + B_0\sqrt{\varepsilon_p}\,exp\left(-\alpha\left(\overset{\circ}{\varepsilon}_p\right)T\right)$$

In this model, σ_a is the thermal component of the flow stress given by

$$\sigma_a = \sigma_g + \frac{k_h}{\sqrt{l}} + K\varepsilon_p^n$$

where σ_g is the contribution due to solutes and initial dislocation density, k_h is the microstructural stress intensity, l is the average grain diameter, K is zero for fcc materials, B, B_0 are material constants. In the thermally activated terms, the functional forms of the exponents α and β are

$$\alpha = \alpha_0 - \alpha_1 ln\left(\overset{\circ}{\varepsilon}_p\right), \quad \beta = \beta_0 - \beta_1 ln\left(\overset{\circ}{\varepsilon}_p\right)$$

where $\alpha_0, \alpha_1, \beta_0, \beta_1$ are material parameters that depend on the type of material (fcc, bcc, hcp, alloys). The Zerilli-Armstrong model has been modified by for better performance at high temperatures.

2.2.4 Mechanical threshold stress flow stress model

A more complex model that is based on ideas from dislocation dynamics is the Mechanical Threshold Stress (MTS) model. This model has been used to model the plastic deformation of copper, tantalum, alloys of steel, and aluminum alloys. However, the MTS model is limited to strain-rates less than around 10^7/s.

$$\sigma_y\left(\varepsilon_p, \overset{\circ}{\varepsilon}_p, T\right) = \sigma_a + \left(\sigma_i\sigma_i + S_e\sigma_e\right)\frac{\mu\left(p, T\right)}{\mu_0}$$

where σ_a is the thermal component of mechanical threshold stress, σ_i is the component of the flow stress due to intrinsic barriers to thermally activated dislocation motion and dislocation-dislocation interactions, σ_e is the component of the flow stress due to microstructural evolution with increasing deformation (strain hardening), (S_i, S_e) are temperature and strain-rate dependent scaling factors, and μ_0 is the shear modulus at 0 K and ambient pressure.

The scaling factors take the Arrhenius form

$$s_i = \left[1 - \left(\frac{k_b T}{g_{0i} b^3 \mu\left(p, T\right)} ln \frac{\mathring{\varepsilon}_p}{\mathring{\varepsilon}_p}\right)^{1/q_i}\right]^{1/p_i}$$

$$s_e = \left[1 - \left(\frac{k_b T}{g_{0e} b^3 \mu\left(p, T\right)} ln \frac{\mathring{\varepsilon}_p}{\mathring{\varepsilon}_p}\right)^{1/q_e}\right]^{1/p_e}$$

where k_b is the Boltzmann constant, b is the magnitude of the Burgers' vector, (g_{0i}, g_{0e}) are normalized activation energies, $(\mathring{\varepsilon}_p, \mathring{\varepsilon}_p)$ are constant reference strain-rates, and (q_i, p_i, q_e, p_e) are constants. The strain hardening component of the mechanical threshold stress (σ_e) is given by an empirical modified Voce law

$$\frac{d\sigma_e}{d\varepsilon_p} = \theta\left(\sigma_e\right)$$

where,

$$\theta\left(\sigma_e\right) = \theta_0\left[1 - F\left(\sigma_e\right)\right] + \theta_{IV} F\left(\sigma_e\right)$$

$$\theta_0 = a_0 + a_1 ln \mathring{\varepsilon}_p + a_2 \sqrt{\mathring{\varepsilon}_p} - a_3 T$$

$$F\left(\sigma_e\right) = \frac{tanh\left(\alpha \frac{\sigma_e}{\sigma_{es}}\right)}{tanh\left(\alpha\right)}$$

$$ln\left(\frac{\sigma_{es}}{\sigma_{0es}}\right) = \left(\frac{kT}{g_{0es} b^3 \mu\left(p, T\right)}\right) ln\left(\frac{\mathring{\varepsilon}_p}{\mathring{\varepsilon}_p}\right)$$

and θ_0 is the hardening due to dislocation accumulation, θ_{IV} is the contribution due to stage-IV hardening, $(a_0, a_1, a_2, a_3, \alpha)$ are constants, σ_{es} is the stress at zero strain hardening rate, σ_{0es} is the saturation threshold stress for deformation at 0 K, g_{0es} is a constant, and $\overset{\circ}{\varepsilon}_p$ is the maximum strain-rate. Note that the maximum strain-rate is usually limited to about 10^7/s.

2.2.5 Preston-Tonks-Wallace flow stress model

The Preston-Tonks-Wallace (PTW) model is also physically based and has a form similar to the MTS model. However, the PTW model has components that can model plastic deformation in the overdriven shock regime (strain-rates greater that 10^7/s). Hence this model is valid for the largest range of strain-rates among the five flow stress models.

The Preston-Tonks-Wallace (PTW) model attempts to provide a model for the flow stress for extreme strain-rates (up to 10^{11}/s) and temperatures up to melt. A linear Voce hardening law is used in the model. The PTW flow stress is given by

$$\sigma_y\left(\varepsilon_p, \overset{\circ}{\varepsilon}_p, T\right) = \left\{A\left[\tau_s + \alpha ln\left[1 - \varphi exp\left(-\beta - \frac{\theta\varepsilon_p}{\alpha\varphi}\right)\right]\right]\right\}\ \mu\left(p, T\right)$$

$$For\ tharmal\ regim\ A = 2\quad and\ For\ shock\ regim\ A = 2\tau_s\mu(p, T)$$

with

$$\alpha = \frac{s_0 - \tau y}{d}\ \ ,\ \ \beta = \frac{\tau_s - \tau_y}{\alpha}\ \ ,\ \ \varphi = exp\left(\beta\right) - 1$$

where τ_s is a normalized work-hardening saturation stress, s_0 is the value of τ_s at 0K, τ_y is a normalized yield stress, θ is the hardening constant in the Voce hardening law, and d is a dimensionless material parameter that modifies the Voce hardening law.

The saturation stress and the yield stress are given by,

$$\tau_s = max\left\{s_0 - \left(s_0 - s_\infty\right) erf\left[k\widehat{T} ln\left(\frac{\gamma\overset{\circ}{\xi}}{\overset{\circ}{\varepsilon}_p}\right)\right],\ so\left(\frac{\overset{\circ}{\varepsilon}_p}{\gamma\overset{\circ}{\xi}}\right)^{s1}\right\}$$

$$\tau_y = max\left\{ y_0 - (y_0 - y_\infty)\, erf\left[k\widehat{T}ln\left(\frac{\gamma\overset{\circ}{\xi}}{\overset{\circ}{\varepsilon}_p}\right)\right]\ , \min\left\{ y_1\left(\frac{\overset{\circ}{\varepsilon}_p}{\gamma\overset{\circ}{\xi}}\right)^{y2},\ so\left(\frac{\overset{\circ}{\varepsilon}_p}{\gamma\overset{\circ}{\xi}}\right)\right\}\ \right\}$$

where,

$$\widehat{T} = T/T_m$$

and s_∞ is the value of τ_s close to the melt temperature, (y_0, y_∞) are the values of τ_y at 0 K and close to melt, respectively, (k, γ) are material constants, (s_1, y_1, y_2) are material parameters for the high strain-rate regime, and ρ is the density and M is the atomic mass.

Chapter 3

Determination of mechanical properties.

3.1 Measurement & Dimensions of Test Specimen

In order to determine mechanical properties like Maximum load, Tensile strength, Elongation, Yield load, yield stress of SS 304 metal sheet having thickness of 1.17 mm , Uniaxial tensile test is carried out on FIE make Universal testing machine, UTES-40,yield is calculated as per ASTM E8 at 5

3.1.1 Test piece preparation

Standard Rectangular Tension Test Specimens, to determine the cross-sectional area, the center width dimension shall be measured to the nearest 0.005 in. (0.13 mm) for the 8-in. (200-mm) gauge length specimen and 0.001 in. (0.025 mm) for the 2-in. (50-mm) gauge length. The center thickness dimension shall be measured to the nearest 0.001 in. for both specimens.
Standard Round Tension Test Specimens to determine the cross-sectional area, the diameter shall be measured at the center of the gauge length to the nearest 0.001 in. (0.025 mm).General-Test specimens shall be either substantially full size or machined,

as prescribed in the product specifications for the material being tested.

Wrongly prepared test specimens often causes unsatisfactory results. It is important,that due care must be taken in preparation of specimens, for accuracy of results.

3.1.2 Dimensions of standard test piece

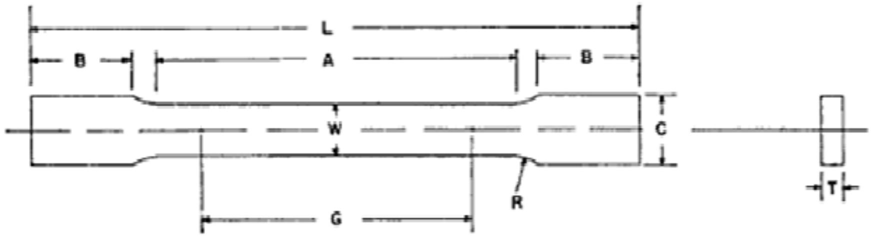

Figure 3.1: Uniaxial Tensile Test Specimen

Table 3.1: Dimensions of Standard Specimens

	Dimensions of Standard Specimen	
	In.	mm
G-Gauge Length	2.000 $\pm$ 0.005	50 $\pm$ 0.10
W-Width	0.500 $\pm$ 0.010	12.5 $\pm$ 0.25
T-Thickness	Thickness of Material	Thickness of Material
R-Radius of fillet, min	0.5	13
L-Overall length, min	8	200
A-Length of reduced section, min	2.25	60
B-Length of grip section, min	2	50
C-Width of grip section, approximate	0.75	20

3.2 Determination of Tensile Properties

3.2.1 Yield Point

Yield Point-Yield point is the first stress in a material, less than the maximum obtainable stress, at which an increase in strain occurs without an increase in stress. Yield point is intended for application only for materials that may exhibit the unique characteristic of showing an increase in strain without an increase in stress. The stress-strain diagram is characterized by a sharp knee or discontinuity.

3.2.2 Yield Strength

Yield strength is the stress at which a material exhibits a specified limiting deviation from the proportionality of stress to strain. The deviation is expressed in terms of strain, percent offset, total extension under load, etc.

3.2.3 Reduction of Area

Fit the ends of the fractured specimen together and measure the mean diameter or the width and thickness at the smallest cross section to the same accuracy as the original dimensions. The difference between the area thus found and the area of the original cross section expressed as a percentage of the original area is the reduction of area.

3.2.4 Tensile Strength

Calculate the tensile strength by dividing the maximum load the specimen sustains during a tension test by the original cross-sectional area of the specimen.

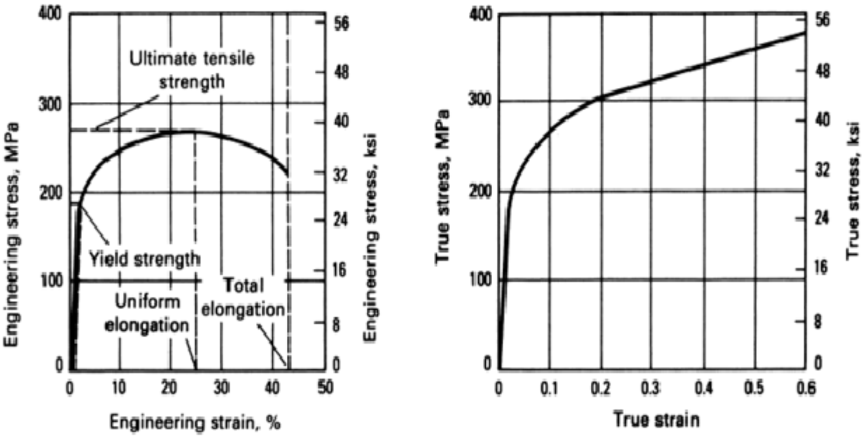

Figure 3.2: Engineering True Stress-Strain Diagram

Table 3.2: Tensile Properties of Tested SS304

No.	**De**	**Area (mm2)**	**Guage Length (mm)**	**Final Length (mm)**	**Yield Load (KN)**	**Ulti. Load (KN)**	**YS N/ mm2**	**UTS N/ mm2**	**Elongation. (%)**	
1	0	12.78X1.17	14.95	50	78.52	5.580	10.720	373	717	57.040
2	45	12.8X1.19	15.232	50	78.42	5.420	9.840	356	646	56.840
3	90	12.7X1.18	14.986	50	77.52	5.660	9.800	378	654	55.040

3.3 Average Tensile Properties of SS 304 tested at rolling direction of $0°, 45°$, and $90°$

Figure 3.3: tensile testing machine and specimens

Table 3.3: Chemical Properties of Tested SS304

Elements	*Percentage*
Carbon	0.057
Sulphur	0.005
Phosphorous	0.035
Silicon	0.320
Manganese	1.100
Chromium	18.100
Nickel	8.100
Molybdenum	0.1000

3.4 Chemical composition of SS 304 sheet tested

Spectro analysis is carried according to ASTM E- 1086-2008

3.5 Determination of n,K,and r Properties

Here a sample calculation is given for sample-1.

For determination of n, true stress & true strain value put on logarithmic scale. At true strain at 1 corresponding true stress value indicate the strength co-efficient K & the slope of straight line that gives the value of n. Similarly all values can be found out for each samples. True stress is given by:

$$\sigma_\tau = \ln(\sigma_E + e)$$

True strain is given by:

$$varepsilon = \ln(1 + e)$$

The characteristic equation for n:

$$\sigma_\tau = K \ \times \ \varepsilon^n = log\sigma_\tau = logK \ \times \ nlog \ \varepsilon$$

The value of n is found out with the linear regression equation as follows:

$$= N\Sigma(xy) \times \Sigma x\Sigma y - \ N\Sigma\left(x^2\right) \ \times (\Sigma x)^2$$

The sample calculation to find out anisotropy is found out as follows:

$$r_\theta = \frac{\ln(\triangle w/w_0)}{\ln(\triangle t/t_0)}$$

3.6 Evaluated properties

Table 3.4: Evaluated Properties

Sample No.	Degree	YS (MPa)	UTS (MPa)	K	r	n
1	0	373	717	1435.275	0.9482	0.2145
2	45	356	646	1490	1.2409	0.2082
3	90	378	654	1439.175	1.2510	0.2135
	Avg.	369	672.33	1454.816	1.14627	0.2120

This values are used for simulation of deep drawing at room temperature.

Chapter 4

Simulation of four stage process at room temperature

4.1 FEA Simulation using Hyper Form 11.0

For simulation using FEA tool HYPER FORM 11.0 following steps are done.

4.1.1 Pre processing

- Import of model as die and blank in IGES format created in PRO-E wild fire 5.

- Meshing of imported die with rigid type of mesh having size 20 and meshing of mesh blank with B-Mesh of size 10 with quad elements .

- Material is created in database using properties obtained from tensile testing like yield strength, Co-efficient of strength, strain hardening exponent, Anisotropy r0, r45, r90, μ, E,etc.

4.1.2 Analysis

- Here material properties are assigned to model and thickness is given using tool setup.
- Using tool setup we can also create punch and binder from die or vice versa.
- Auto process is used to input operating parameters such as punch ideal velocity,forming velocity, binder ideal velocity, binder force, clearance between die and punch bottom, etc., it also auto positions the components at safe distance from each other and calculates the punch and binder travel distance automatically.
- After auto position other process parameters are applied and runes to generate_000 and _001 .rad file which is used for post processing.

4.1.3 Post processing

- In post processing 000 .rad file generated during auto position is solved with RADIOS SOLVER, which generates all the result files like T01- containing all the data of position, load , contact forces,etc.
  A001 to A011 - animation file at definite interval of time which can be seen in hyper view.
  STA- it contains all the data of stress strain produced in component if we want to go for second draw then this file generates the blank of second stage. And other relative files which are useful to view results.

4.2 FEA Simulation of first stage

Figure 4.1 (a)shows the view of first draw product and (b) dimensions of product.

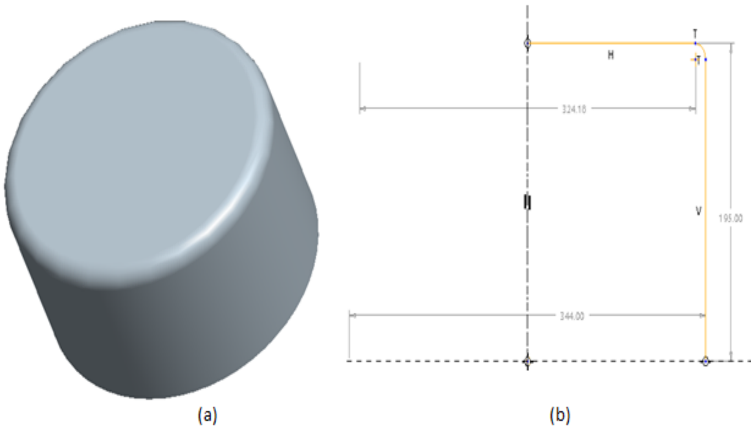

Figure 4.1: First draw product and dimensions.

For first stage simulation mechanical properties obtained by uniaxial tensile testing are used and material is added to database under name SS 304, and properties used are as shown below. Parameters used for the simulation are as given in table 4.1.

Table 4.1: Parameters used for simulation

Yield =369 MPa	Punch Velocity =5000
n = 0.2120	Binding force =769366 N ≈ 100 kg/ cm2
K = 1454.816	Clearance = 10%

Figure 4.2 shows (a) Tool setup in simulation and (b) Transparent view of process.

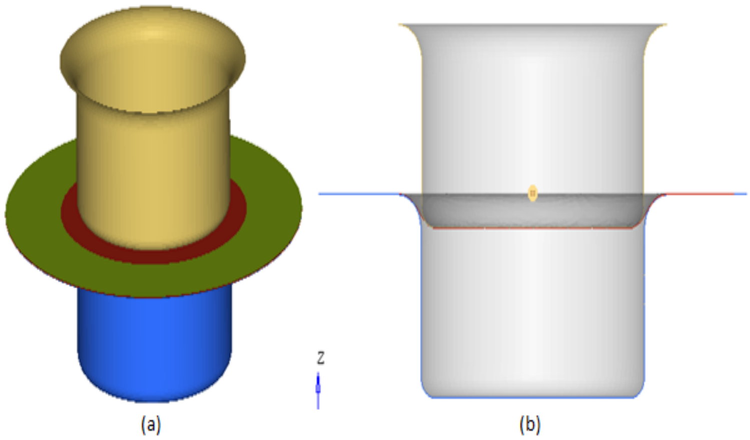

Figure 4.2: (a)Tool setup. (b)Transparent view.

Figure 4.3 shows (a) Component of first stage draw on which two different zones of safe and compression can be seen.and (b) FLD of first draw component which is well within safe region.

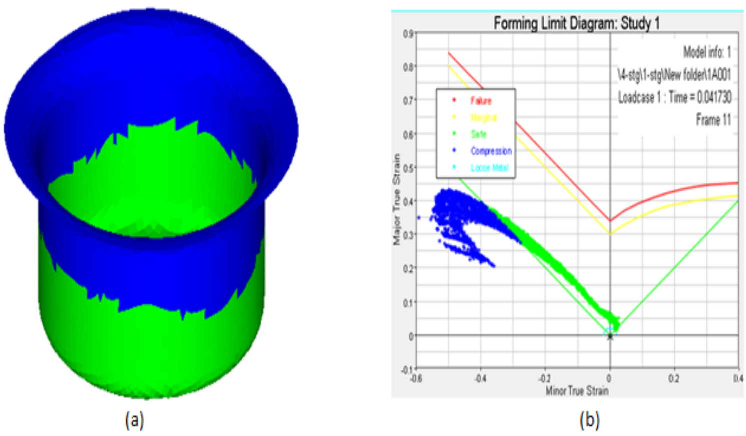

Figure 4.3: (a)Component of first stage draw. (b)FLD of first draw component.

Figure 4.4 (a)shows Percentage thinning in component at end of first draw, which shows maximum thinning is in bottom part and minimum thinning is in flange area where binder holds the blank, (b) shows strain distributions in component at end of first draw.

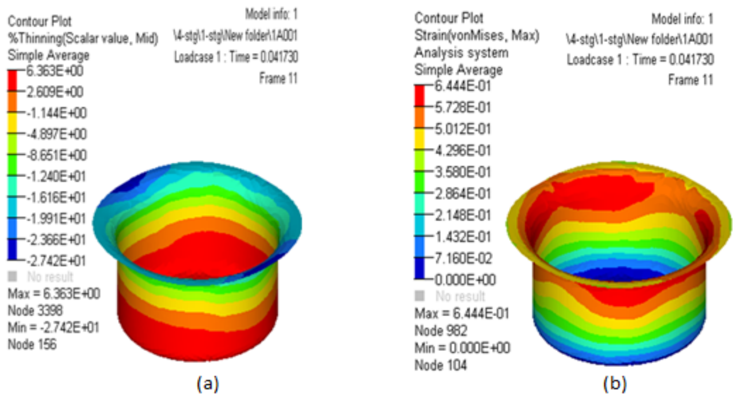

Figure 4.4: (a)Percentage thinning. (b)strain distributions.

Figure 4.5 (a)shows stress distribution in component and (b) shows Thickness distribution in component.

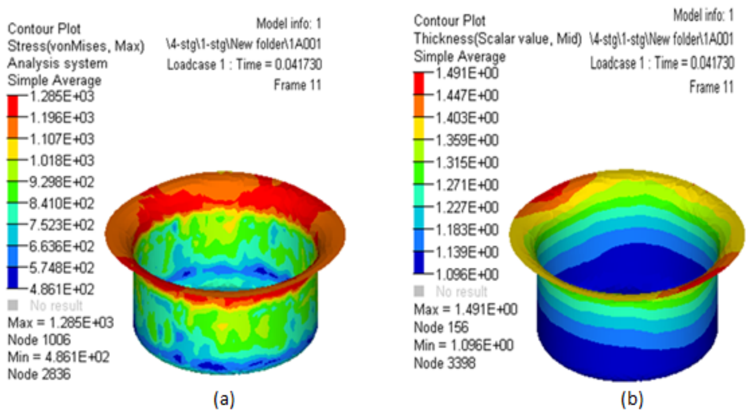

Figure 4.5: (a)stress distribution in component. (b)Thickness distribution in component.

Figure 4.6 (a)Plastic strain distributions in component and (b) shows distribution of Von Mises stress in component.

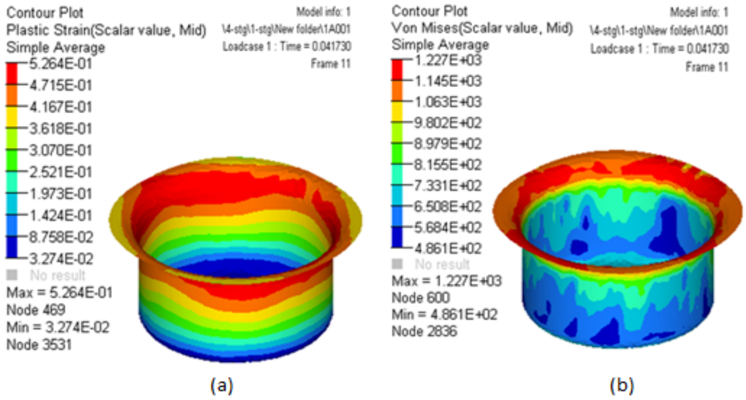

Figure 4.6: (a)Plastic strain distributions in component. (b)distribution of Von Mises stress.

Also, contact force and time required to complete the job is plotted by graph as shown in figure 4.7

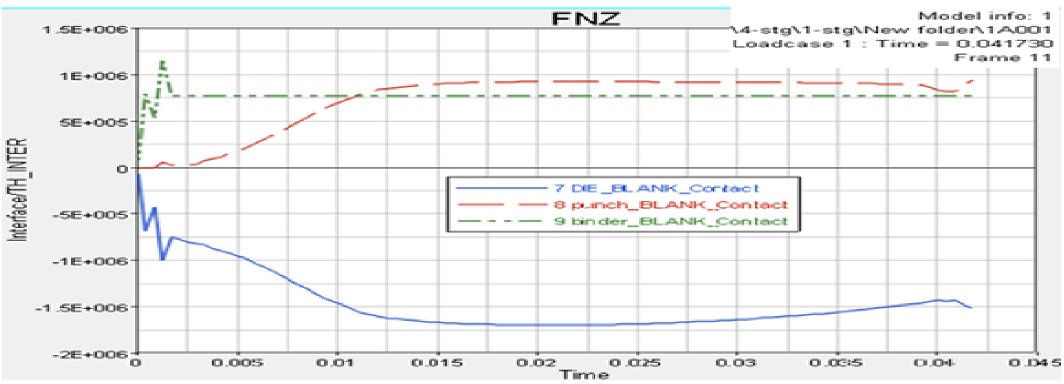

Figure 4.7: contact force and time required

4.3 FEA Simulation of second stage

For the second draw the product of first draw is considered as blank,for this STA file generated in first stage simulation is used which contains all the stress strain data of previous operation.

Parameters used for simulation are given in table4.2

Table 4.2: Parameters used for simulation of second stage

Yield =369 MPa	Punch Velocity =5000
n = 0.2120	Binding force =577024 N ≈ 78 kg/ cm2
K = 1454.816	Clearance = 10%

Figure 4.8 (a) shows the component of second draw and (b) shows dimensions of second draw component.

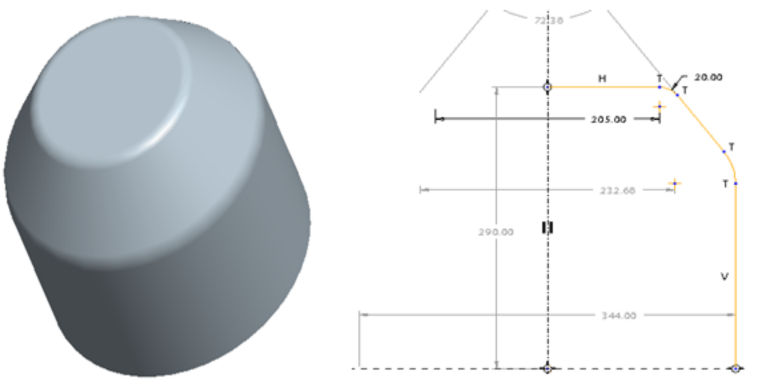

(a) (b)

Figure 4.8: (a)component of second draw and (b)Dimensions of second draw component.

Tool setup used for simulation with pre strained blank is shown in figure 4.9(a), and transparent view is shown in 4.9(b) where product of first draw is used as blank.

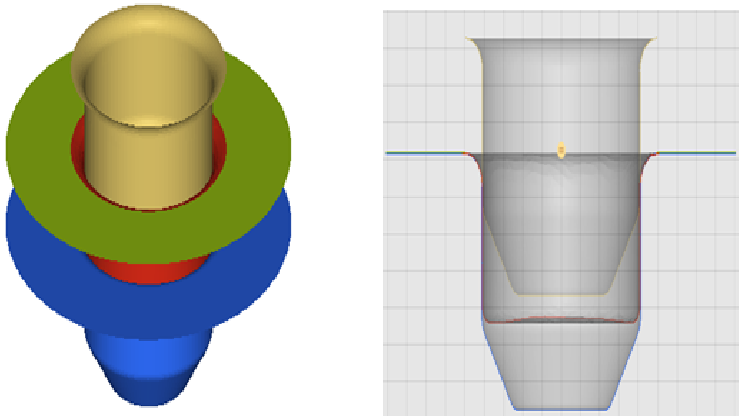

(a) (b)

Figure 4.9: (a)Tool setup for second draw (b)transparent view.

FLD obtained from simulation using parameters shown in table 4.2 is shown in figure 4.10(b) and figure 4.10(a) shows component after second draw.

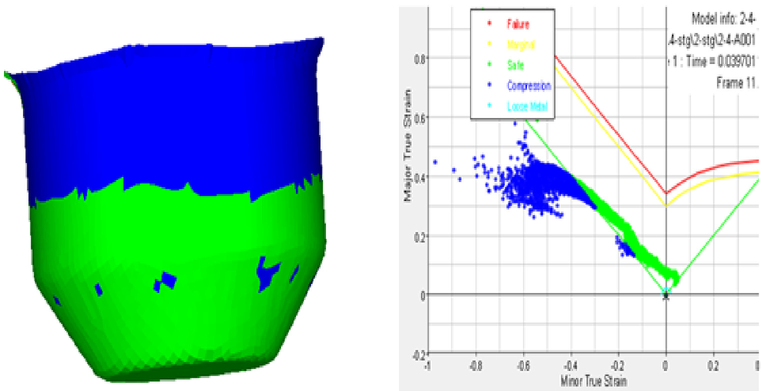

(a) (b)

Figure 4.10: (a)component after second draw. (b)FLD of second draw product.

Figure 4.11 (a) shows maximum and minimum percentage thinning in second drawn component and figure (b) shows strain distribution in component.

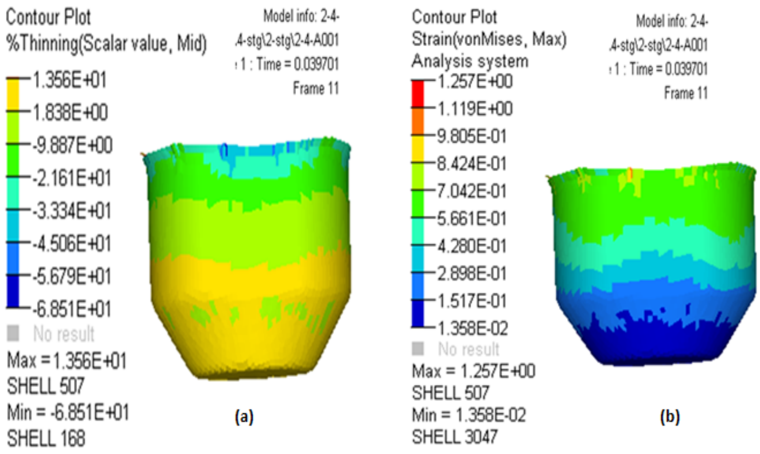

Figure 4.11: (a)percentage thinning in second draw. (b)strain distribution.

Stress and thickness distribution of second drawn product is shown in fig 4.12(a) and 4.12(b).

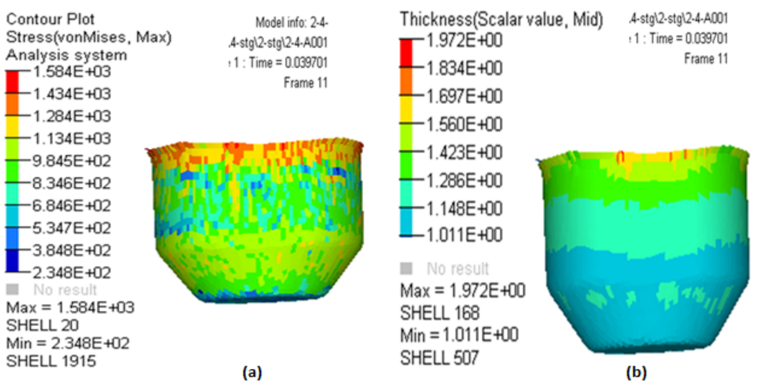

Figure 4.12: (a)thickness distribution in second draw. (b)strain distribution in second draw.

Also, the plastic strain and Von Mises stress distribution is as shown in figure 4.13 (a) and 4.13(b).

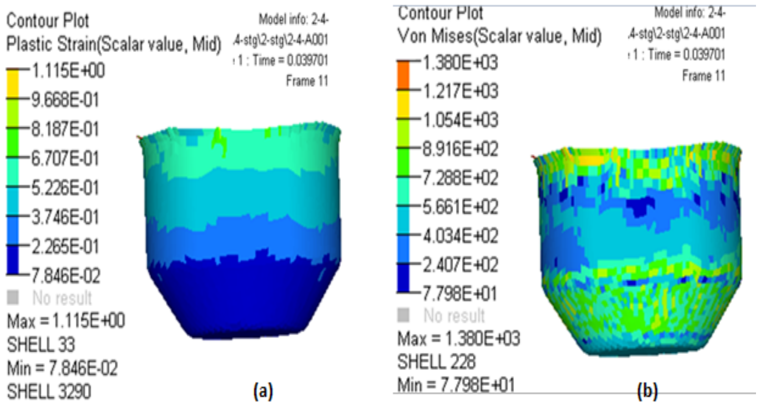

Figure 4.13: (a)plastic strain distribution in second draw. (b)Von Mises distribution in second draw.

Contact forces between die, blank and punch with time required to draw the component is shown in figure 4.14.

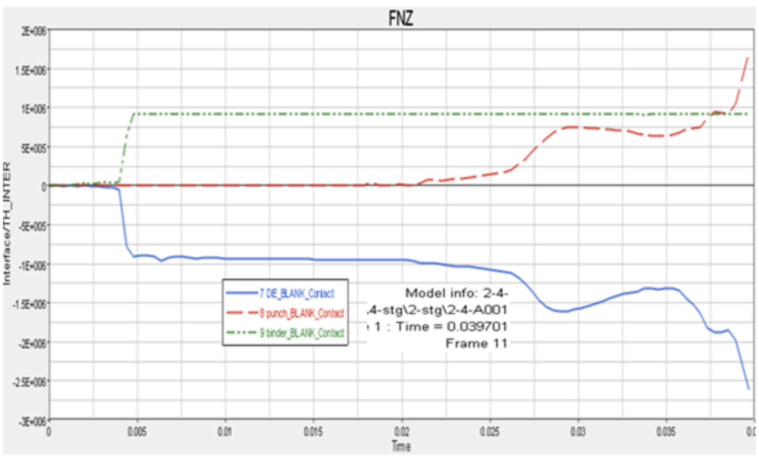

Figure 4.14: Contact forces and time required for second draw.

4.4 FEA Simulation of direct second stage

attempt was made to combine the first two stages of the process with properties obtained at room temperature and results obtained are shown below.
the die and punch were same as they were used for second draw, but a fresh blank is used to simulate the drawing process. Parameters used for simulation are as shown in table 4.3 below.

Table 4.3: Parameters used for simulation direct second stage

Yield =369 MPa	Punch Velocity =5000
n = 0.2120	Binding force =769366 N ≅ 100 kg/ cm2
K = 1454.816	Clearance = 10%

figure 4.15(a) shows tool setup used and 4.15(b) shows the transparent view of the process.

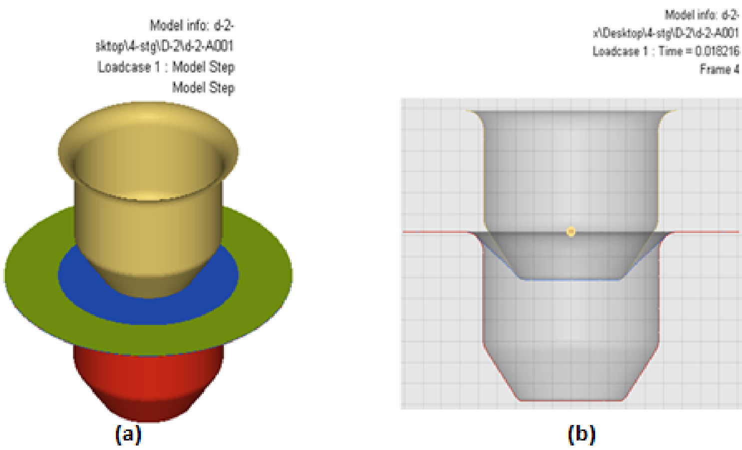

Figure 4.15: (a) Tool setup, (b) Transparent view.

FLD of the component drawn drawn in one stage is shown in figure 4.16 (b), and 4.16(a) shows component formed in one stage. Percentage of thinning in component

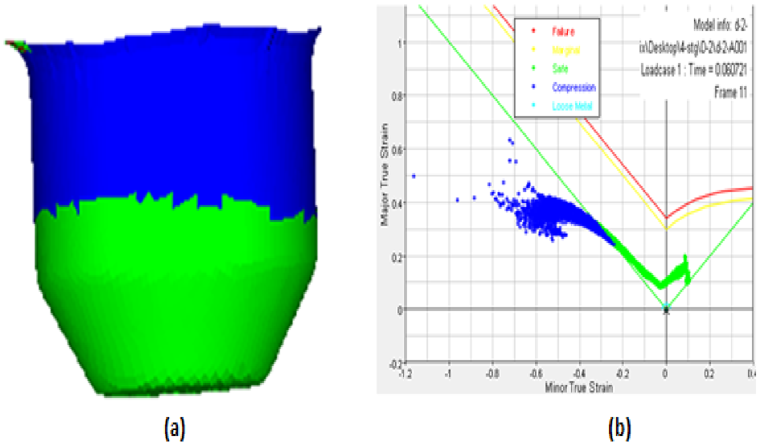

Figure 4.16: (a) First draw component, (b) FLD of first draw component.

given by simulation is shown in figure 4.17(a), and figure 4.17(b) shows strain distribution in component.

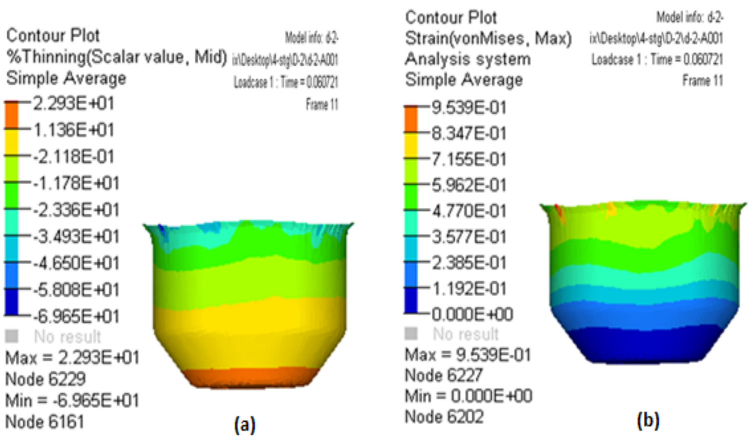

Figure 4.17: (a) Percentage of thinning, (b) strain distribution.

figure 4.18(a) shows stress distribution and figure 4.18(b) shows thickness distribution.

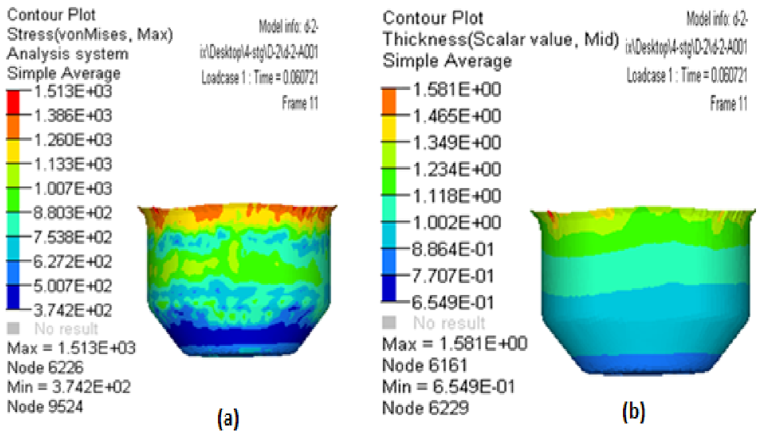

Figure 4.18: (a) stress distribution, (b) thickness distribution.

Plastic strain distribution is shown in figure 4.19(a), and Von Mises stress distribution is shown in figure 4.19(b) for the component drawn in one stage.

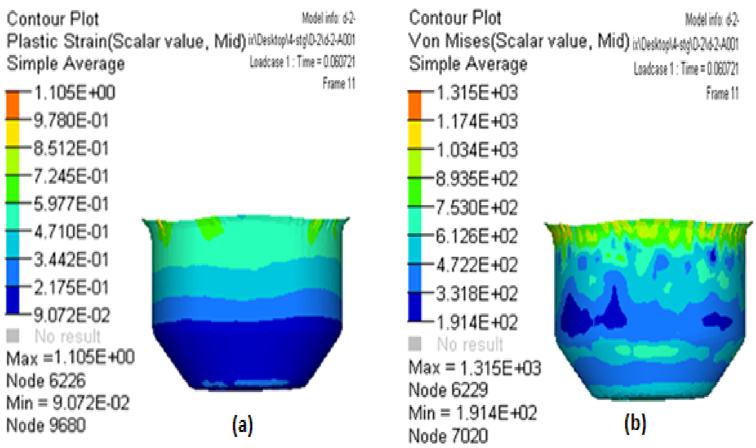

Figure 4.19: (a) Plastic strain distribution, (b) Von Mises distribution.

also the time require to draw the component in one stage with contact forces of punch, blank and die is shown in figure 4.20

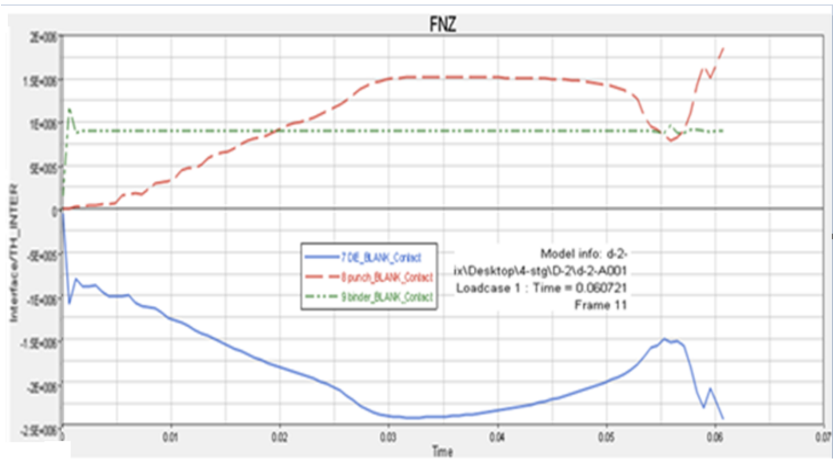

Figure 4.20: Contact forces between die, punch and blank with time required to draw the component.

4.5 FEA Simulation of direct third stage

also, attempt was made to form the third stage product in one stage at atmospheric temperature and results obtained are shown below.
figure 4.21 (a) shows the component of third stage and figure 4.21(b) shows dimension of component.

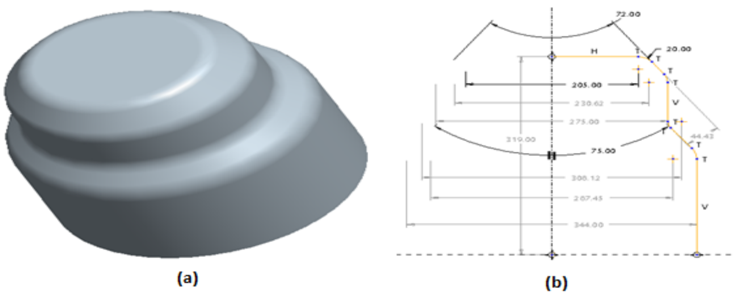

Figure 4.21: (a)component, (b) dimension of component.

Parameters used for simulation of direct third stage are as shown in table 4.4 below.

Table 4.4: Parameters used for simulation direct third stage

Yield =369 MPa	Punch Velocity =2500
n = 0.2120	Binding force =491298 N ≅ 60 kg/ cm2
K = 1454.816	Clearance = 10%

figure 4.22(a) shows tool setup used for simulation and figure 4.22(b) shows transparent view of process.

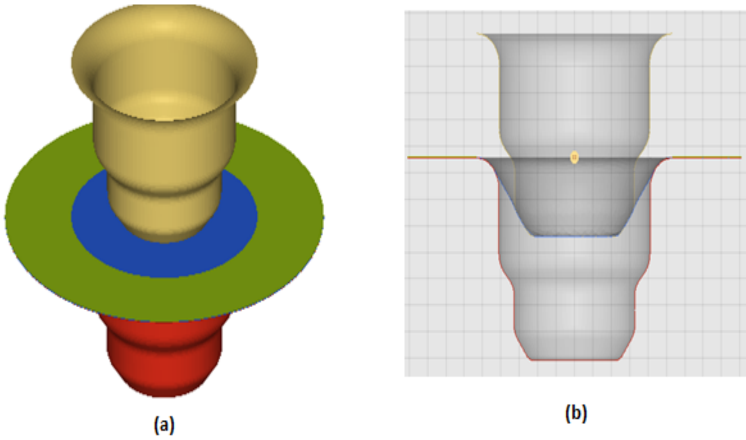

Figure 4.22: (a)Tool setup, (b) Transparent view.

figure 4.23(a) Third draw component in one step and figure 4.23(b) FLD of one step process.

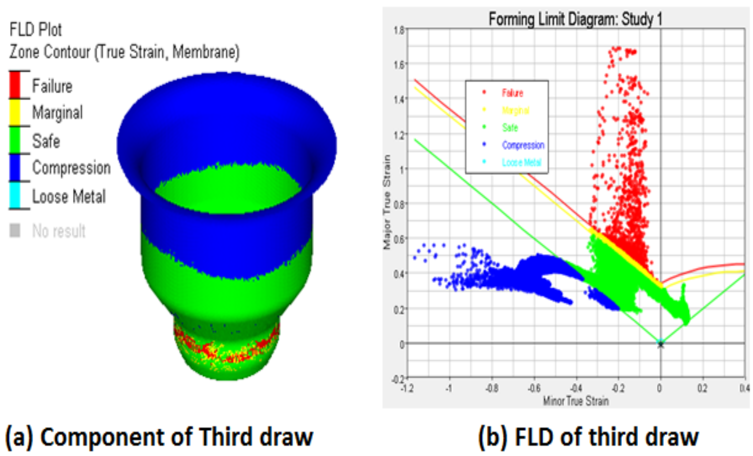

Figure 4.23: (a)one step component, (b) FlD of one step.

figure 4.24(a) shows percentage thinning in component 4.24(b) Strain distribution in component.

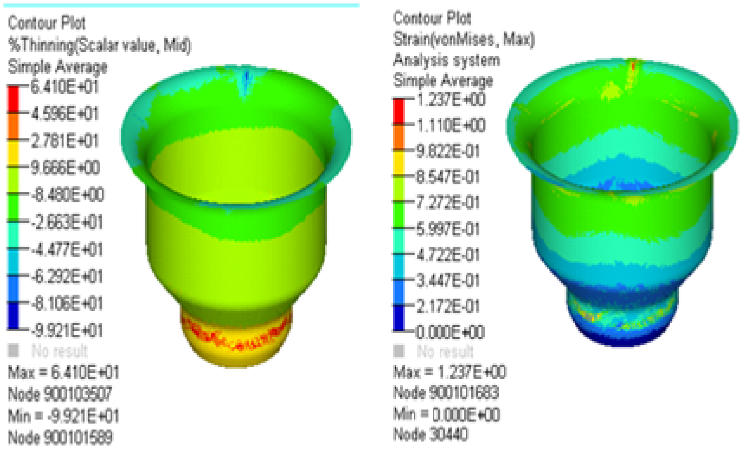

Figure 4.24: (a)percentage thinning in component, (b) Strain distribution in component.

figure 4.25(a) shows stress distribution in component 4.25(b) shows thickness distribution in component.

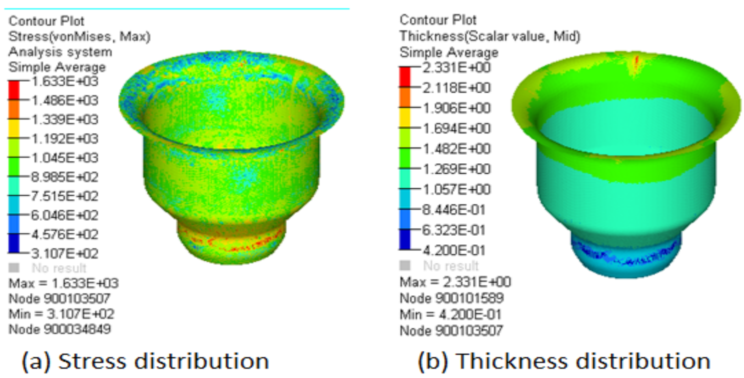

Figure 4.25: (a)percentage thinning in component, (b) Strain distribution in component.

figure 4.26(a) shows Plastic strain distribution in component 4.26(b) shows Von Mises distribution in component.

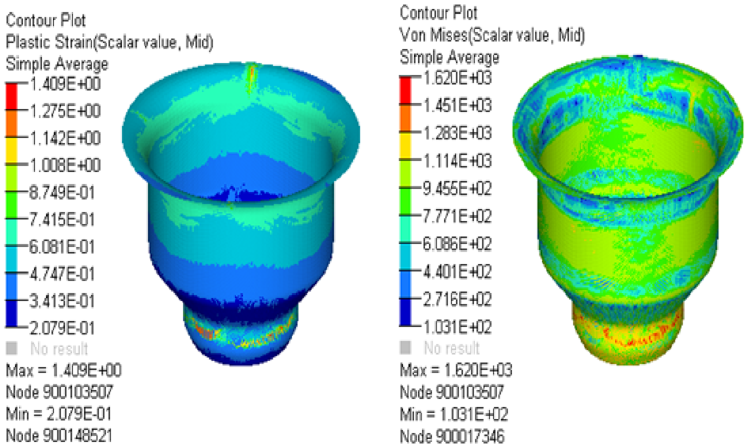

Figure 4.26: (a)Plastic strain distribution in component, (b) Von Mises distribution in component.

figure 4.27 shows contact force between punch, die and blank along with time required to draw the component

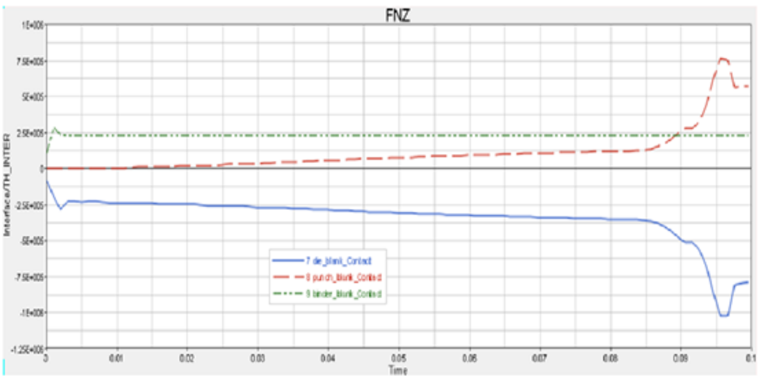

Figure 4.27: Contact forces and time required.

Chapter 5

Determination of mechanical properties at 120° C temperature.

5.1 Measurement & Dimensions of Test Speciman

In order to determine mechanical properties like Maximum load, Tensile strength, Elongation, Yield load, yield stress of SS 304 metal sheet having thickness of 1.17 mm at 120° C., Uniaxial tensile test is carried out on FIE make Universal testing machine, UTES-40, with a induction heating and temperature control attachment which uses three thermocouple to measure temperature. For testing ASTM E21:2009 standard is used which is for measuring mechanical properties at elevated as well as negative temperature, standard doesn't include strain rate sensitivity.

In reference to standard soaking time of 20Mins are provided in order to ensure uniform temperature distribution and time required to achieve temperature was 1 hour, details of test specimen preparation is discussed below.

5.1.1 Test piece preparation

Standard Rectangular Tension Test Specimens, to determine the cross-sectional area, the center width dimension shall be measured to the nearest 0.005 in. (0.13 mm)

for the 8-in. (200-mm) gauge length specimen and 0.001 in. (0.025 mm) for the 2-in. (50-mm) gauge length. The center thickness dimension shall be measured to the nearest 0.001 in. for both specimens.
Standard Round Tension Test Specimens to determine the cross-sectional area, the diameter shall be measured at the center of the gauge length to the nearest 0.001 in. (0.025 mm).General-Test specimens shall be either substantially full size or machined, as prescribed in the product specifications for the material being tested.
Wrongly prepared test specimens often causes unsatisfactory results. It is important,that due care must be taken in preparation of specimens, for accuracy of results.

5.1.2 Dimensions of standard test piece

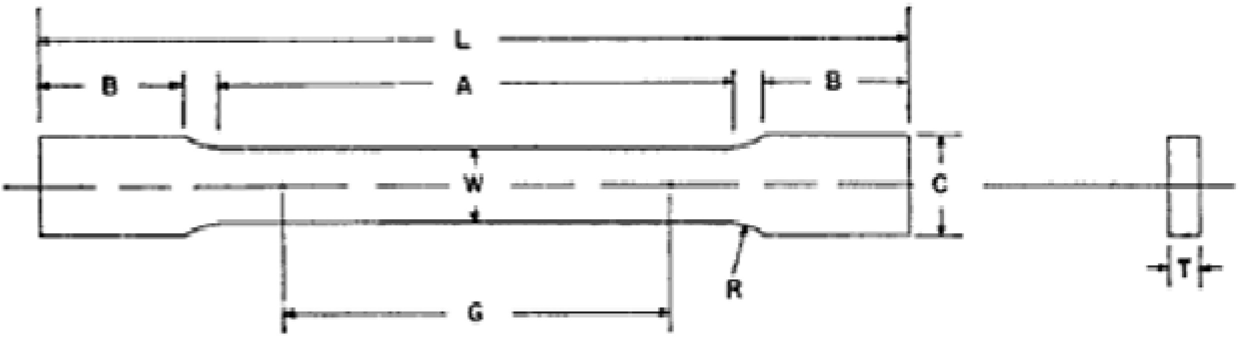

Figure 5.1: Uniaxial Tensile Test Specimen

5.2 Average Tensile Properties of SS304 tested at rolling direction of $0°, 45°$, and $90°$

Table 5.1: Dimensions of Standard Specimens

	Dimensions of Standard Specimen	
	In.	mm
G-Gauge Length	2.000 $\pm$ 0.005	50 $\pm$ 0.10
W-Width	0.500 $\pm$ 0.010	12.5 $\pm$ 0.25
T-Thickness	Thickness of Material	Thickness of Material
R-Radius of fillet, min	0.5	13
L-Overall length, min	8	200
A-Length of reduced section, min	2.25	60
B-Length of grip section, min	2	50
C-Width of grip section, approximate	0.75	20

Table 5.2: Tensile Properties of Tested SS304

No.	**De**	**Area (mm2)**	**Guage Length (mm)**	**Final Length (mm)**	**Yield Load (KN)**	**Ulti. Load (KN)**	**YS N/ mm2**	**UTS N/ mm2**	**Elongation. (%)**	
1	0	12.78X1.17	14.95	50	68.70	4.920	7.760	325.3	513.1	37.40
2	45	12.8X1.19	15.232	50	68.50	5.320	7.840	349.1	514.4	37.00
3	90	12.7X1.18	14.986	50	66.90	5.120	8.760	335.9	574.7	33.80

5.3 Chemical composition of SS 304 sheet tested

Spectro analysis is carried according to ASTM E- 1086-2008

5.4 Determination of n,K,and r Properties

Here a sample calculation is given for sample-1.

For determination of n, true stress & true strain value put on logarithmic scale. At true strain at 1 corresponding true stress value indicate the strength co-efficient K & the slope of straight line that gives the value of n. Similarly all values can be found

Table 5.3: Chemical Properties of Tested SS304

Elements	*Percentage*
Carbon	0.057
Sulphur	0.005
Phosphorous	0.035
Silicon	0.320
Manganese	1.100
Chromium	18.100
Nickel	8.100
Molybdenum	0.1000

out for each samples. True stress is given by:

$$\sigma_\tau = \ln\left(\sigma_E + e\right)$$

True strain is given by:

$$varepsilon = \ln\left(1 + e\right)$$

The characteristic equation for n:

$$\sigma_\tau = K \ \times \ \varepsilon^n = log\sigma_\tau = logK \ \times \ nlog\ \varepsilon$$

The value of n is found out with the linear regression equation as follows:

$$= N\Sigma\left(xy\right) \times \Sigma x \Sigma y - \ N\Sigma\left(x^2\right) \ \times \left(\Sigma x\right)^2$$

The sample calculation to find out anisotropy is found out as follows:

$$r_\theta = \frac{\ln(\triangle w/w_0)}{\ln(\triangle t/t_0)}$$

5.5 Evaluated properties

Table 5.4: Evaluated Properties

Sample No.	Degree	YS (MPa)	UTS (MPa)	K (MPa)	r	n
1	0	325.3	513.1	1020.095	0.8328	0.1876
2	45	349.1	514.4	1017.241	1.1482	0.1966
3	90	335.9	574.7	1016.471	1.1568	0.1851
	Avg.	336.766	534.046	1017.917	1.04593	0.1897

Thus this values are used to simulate warm deep drawing condition.

Chapter 6

Simulation of warm deep drawing.

In order to reduce the number of stages required further simulation of third stage of original process is done using mechanical properties obtained by tensile testing at 120 C, and properties used is as given in table 6.1 below.

Table 6.1: Properties used for warm simulation of direct third stage

Yield =336 MPa	Punch Velocity =2500
n = 0.1897	Binding force =491298 N ≅ 60 kg/ cm2
K = 1017.917	Clearance = 10%

figure 6.1 (a) shows the component of third stage and figure 6.1(b) shows dimension of component. Results obtained are as shown in figures below.

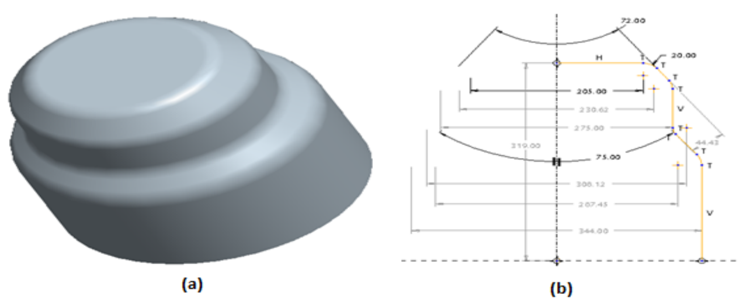

Figure 6.1: (a)component, (b) dimension of component.

figure 6.2(a) shows tool setup used for simulation and figure 60.2(b) shows transparent view of process. Results obtained using following parameters are shown below.

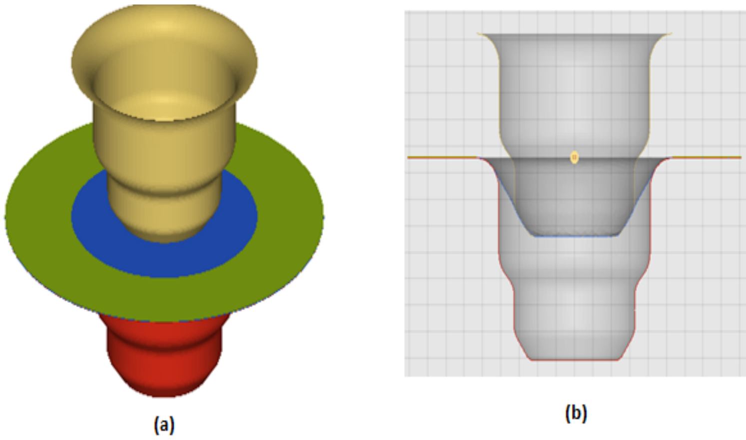

Figure 6.2: (a)Tool setup, (b) Transparent view.

Figure 6.3(a) shows component made in one stage using temperature, and figure 6.3(b) shows FLD obtained from the simulation.

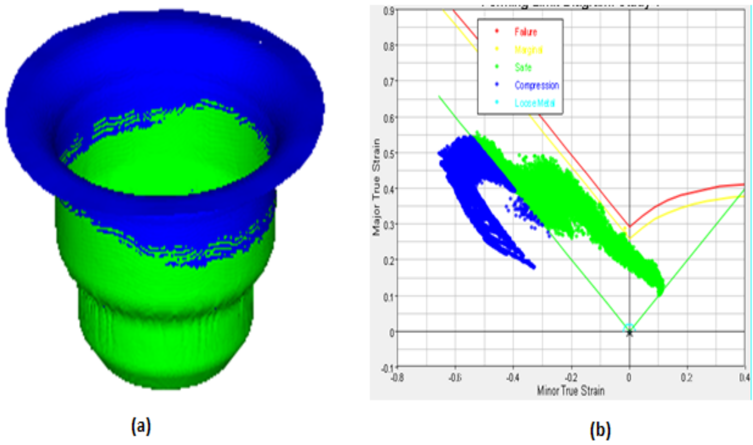

Figure 6.3: (a)first draw component, (b) FLD using temperature for first draw.

Figure 6.4(a) shows percentage of thinning obtained in component for first stage using temperature, and figure 6.4(b) shows strain distribution in component.

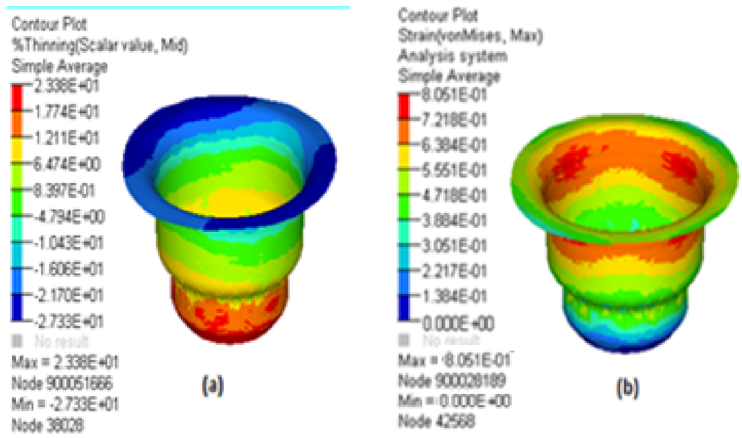

Figure 6.4: (a)percentage thinning, (b) strain distribution.

Figure 6.5(a) shows distribution of stress in component and Figure 6.5(b) shows distribution of thickness in component.

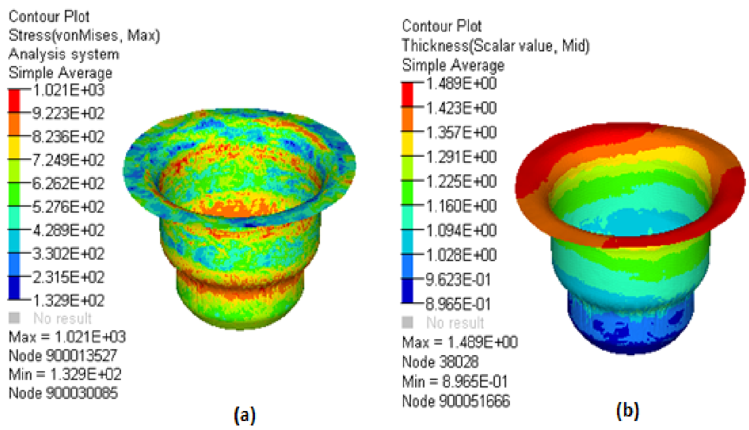

Figure 6.5: (a)Stress distribution, (b) Thickness distribution.

Figure 6.6(a) shows Plastic strain distribution in component and Figure 6.6(b) shows Von Mises distribution of thickness in component. Also the contact forces

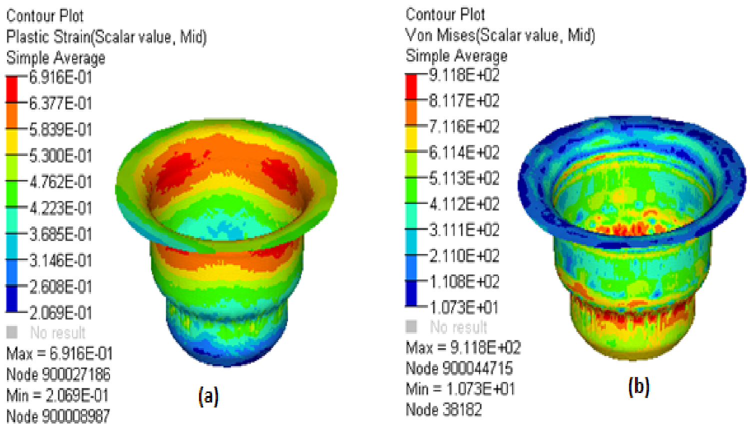

Figure 6.6: (a)Plastic strain distribution, (b) Von Mises distribution.

between die,blank, and punch are shown with time required to draw the product in one stage using temperature in figure 6.7.

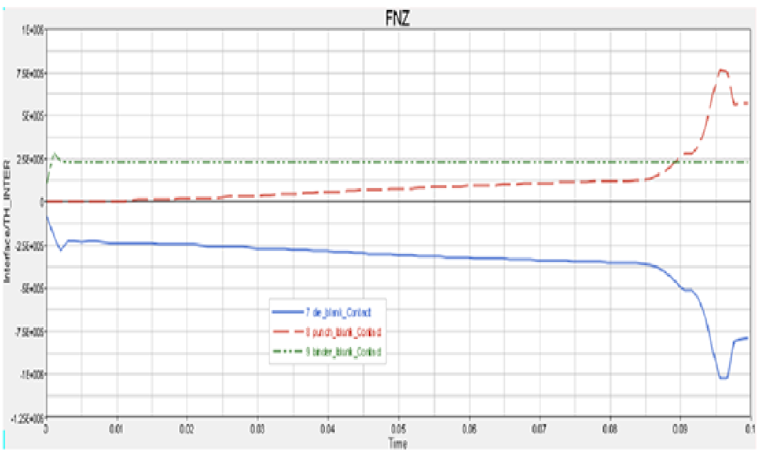

Figure 6.7: contact forces and time required.

Chapter 7

Results and discussion

7.1 Uniaxial tensile testing

7.1.1 tensile testing at room temperature

Figure 7.1 shows true stress strain diagram on logarithmic scale for sample along 0° where value of n is 0.2145 and value of K is 1453.275.

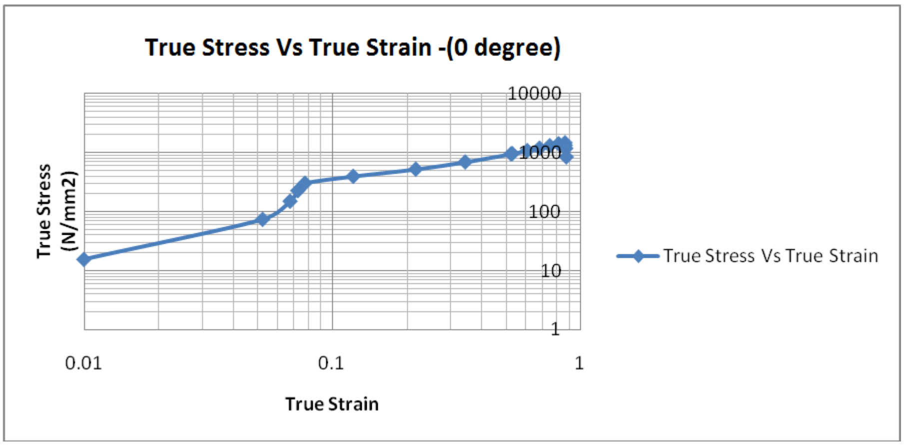

Figure 7.1: True stress Vs True Strain diagram for 0° sample

Figure 7.2 shows true stress and true strain diagram on logarithmic scale for sample along 45° where value of n is 0.2082 and k is 1490.

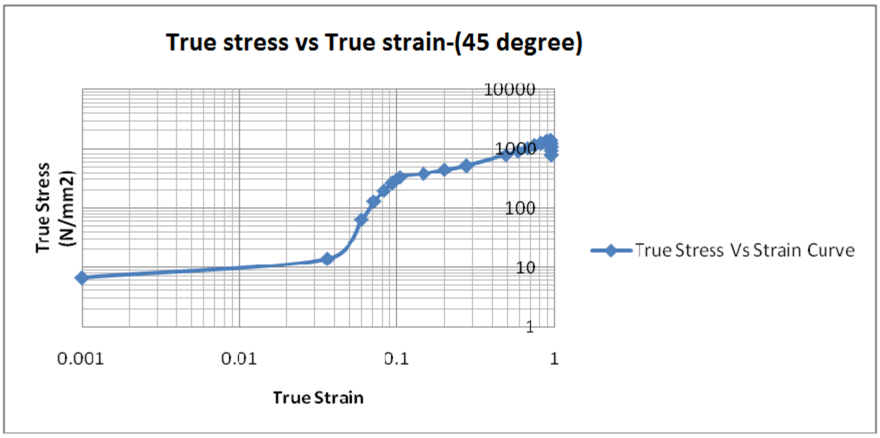

Figure 7.2: True stress Vs True Strain diagram for 45° sample

Figure 7.3 shows true stress Vs strain diagram on logarithmic scale for sample along 90° where value of n is 0.2135 and value of K is 1439.175.

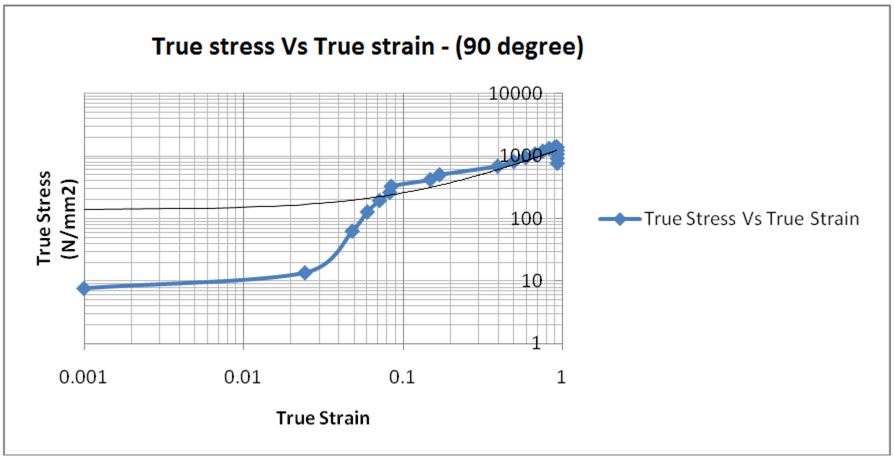

Figure 7.3: True stress Vs True Strain diagram for 90° sample

7.1.2 tensile testing at 120° C temperature

Figure 7.4 shows true stress strain diagram on logarithmic scale for sample along 0° where value of n is 0.1876 and value of K is 1020.095.

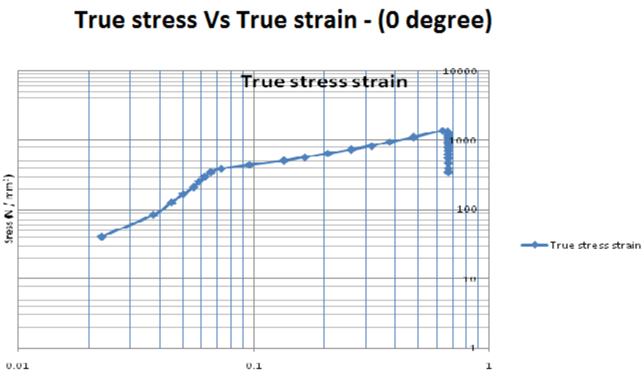

Figure 7.4: True stress Vs True Strain diagram for 0° sample

Figure 7.5 shows true stress strain diagram on logarithmic scale for sample along 45° where value of n is 0.1966 and value of K is 1017.214 .

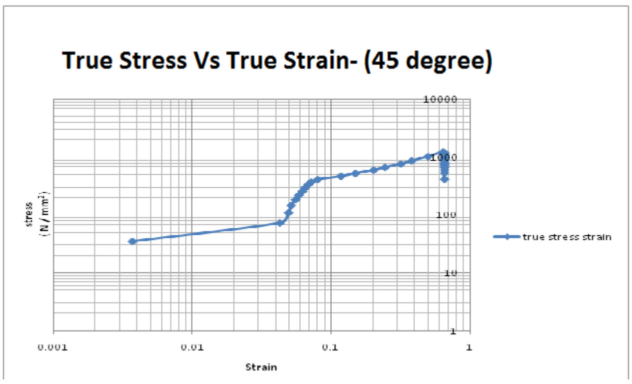

Figure 7.5: True stress Vs True Strain diagram for 45° sample

Figure 7.6 shows true stress strain diagram on logarithmic scale for sample along 90° where value of n is 0.1851 and value of K is 1016.417.

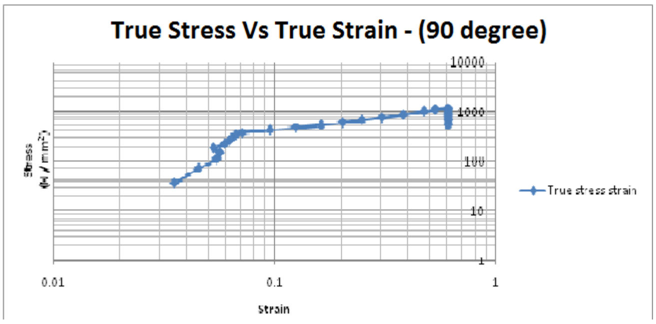

Figure 7.6: True stress Vs True Strain diagram for 90° sample

- Comparison of results obtained from From tensile testing.

Table 7.1: Comparison of mechanical properties

Temp.	Rolling direction	Yield load	Yield strength	Ultimate load	Ultimate strength	Strain hardening exponent	Co-efficient of Strength	% elongation
Room temp.	0°	5580	373	10720	717	0.2145	1435.275	57.040
120° C	0°	4920	325.3	7760	513.1	0.1876	1020.095	37.40
Room temp.	45°	5660	378	9800	646	0.2082	1490	56.840
120° C	45°	5320	349.1	7840	514.4	0.1966	1017.241	37.00
Room temp.	90°	5420	356	9840	654	0.2135	1439.175	55.040
120° C	90°	5120	335.9	8760	574.7	0.1851	1016.917	33.80

Here from the results of tensile testing at room temperature and 120°C it is clearly seen that with increase in temperature values of mechanical properties especially n and k which are important values from draw ability point of view.

7.2 Simulation results.

here the results obtained in simulation of process at room temperature as well as at 120°C are shown and discussed.

- Results of first stage simulation are shown in table 7.2.

Table 7.2: Results from simulation of first stage at room temperature

Parameter	Minimum	Maximum
% Thinning	-2.742E+01	6.363E+00
Strain	0.0000E+00	6.444E-01
Stress	4.861E+02	1.285E+03
Thickness	1.096E+00	1.491E+00
Plastic Strain	3.274E-02	5.26E-01
Von Mises	4.861E+02	1.227E+03
Punch-Blank force	-	9.8E+05
Time of process	-	0.042

Result shows that maximum percentage of thinning is 6.3% only.

Punch force required to draw the product in first stage is approximately 9.8E05.

Time required to complete the stage is 2.52 seconds.

- Results of second stage simulation are shown in table 7.3.

Table 7.3: Results from simulation of second stage at room temperature

Parameter	Minimum	Maximum
% Thinning	-6.851E+01	1.356E+01
Strain	1.358E-02	1.257E+00
Stress	2.348E+02	1.584E+03
Thickness	1.011E+00	1.972E+00
Plastic Strain	7.846E-02	1.115E+00
Von Mises	7.798E+01	1.380E+03
Punch-Blank force	-	1.6E+006
Time of process	-	0.039

Result shows Maximum percentage of thinning is 13.56%.

Punch force required to draw the second stage is 1.6E6, which has increased significantly from the force required in first stage which is the significance of strain hardening in component.

Time required to complete the process is sum of first stage and second stage which is total 4.86 seconds.

- Results obtained from direct second stage simulation at room temperature.

Result shows maximum percentage of thinning is 22.93%.

Table 7.4: Results from simulation of direct second stage at room temperature

Parameter	Minimum	Maximum
% Thinning	-6.965E+01	2.293E+01
Strain	0.000E+00	9.539E-01
Stress	3.742E+02	1.513E+03
Thickness	6.549E-01	1.581E+00
Plastic Strain	9.072E-02	1.105E+00
Von Mises	1.914E+02	1.315E+03
Punch-Blank force	-	1.7E+06
Time of process	-	0.06

Punch force required to draw the component is 1.7E+06 which is nearly equal to force required to draw the component of second draw, but because of increase in length the maximum percentage of thinning increases from 13.56 to 22.93, which shows the effect of stages used in production.

Also the time required to draw the component is 3.6 seconds which is less than time required for product manufactured in two stages.

- Results obtained from direct third stage simulation at room temperature.

Table 7.5: Results from simulation of direct third stage at room temperature

Parameter	Maximum	Minimum
% Thinning	6.410E+01	-9.921E+01
Strain	1.237E+00	0.000E00
Stress	1.633E+03	3.107E+02
Thickness	2.331E-00	4.200E-01
Plastic Strain	1.409E+00	2.079E-01
Von Mises	1.620E+03	1.031E+02
Punch-Blank force	-	1.9E+06
Time of process	-	0.0098

Simulation results of direct third stage product in one step at room temperature shows failure in the bottom of component within the length of 21 mm.

Maximum Percentage of thinning is 64.10% which is far beyond the acceptance criterion.

Also the punch blank contact force significantly increases to 1.9E6 because of strain hardening.

Thus from simulation it is clear that component of third stage can not be drawn in one step at room temperature.

In order to draw the component of third stage in one step properties obtained by hot tensile testing are used and results obtained are discussed. • Results obtained from direct third stage product simulation with 120° C temperature.

Table 7.6: Results from simulation of direct third stage product with 120°C temperature

Parameter	Minimum	Maximum
% Thinning	-2.733E+01	2.336E+01
Strain	0.000E00	8.051E-01
Stress	1.329E+02	1.021E+03
Thickness	8.956E-01	1.489E+00
Plastic Strain	2.069E-01	6.916E-01
Von Mises	1.073E+01	9.118E+02
Punch-Blank force	-	7.8E5
Time of process	-	0.098

Results obtained by simulation of third stage product of original process in one stage using properties of hot tensile testing shows maximum percentage of thinning is 23.36%. This is due to increase in length of component by 30 mm.

Punch load required to draw the component using hot properties is 7.8E5 which is much less than force required to draw the component of first stage 9.8E5, which shows effect of K, as with temperature value of k is reduced.

Time required to draw the third stage component in one stage using hot properties is 5.88 seconds.

7.3 Effect of various process parameters on warm deep drawing process.

• Effect of blank holding force value is 620580 N and all other parameters are constant is shown in figure 7.7

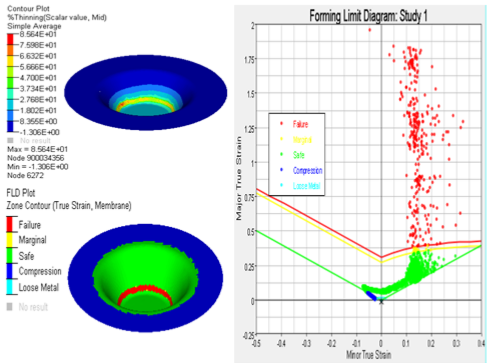

Figure 7.7: True stress Vs True Strain diagram for 90° sample

It is seen that % of thinning increases drastically to 85.64%, also FlD shows failure at punch radius.

- Effect of Punch velocity when value 6000 mm/sec keeping all other parameters same is shown in figure 7.8.

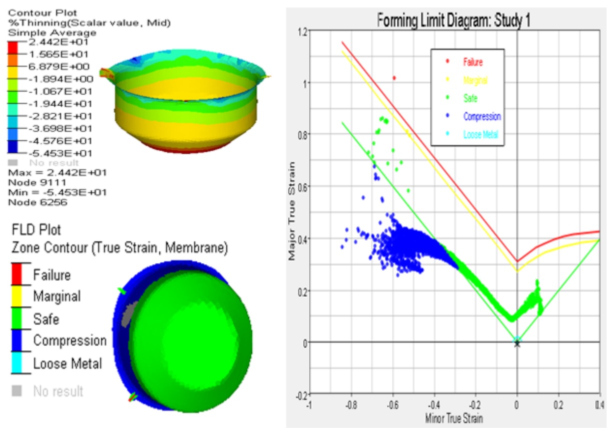

Figure 7.8: True stress Vs True Strain diagram for 90° sample

Results shows Maximum % of thinning as 24% and FLD shows a point going out of Forming limit at die radius.

Thus we can say that FEA analysis is a very powerful tool that can be used in order to save time and cost of experimentation.

Chapter 8

Conclusion and Future scope

8.1 Conclusion

Here an attempt is made to simulate the warm deep drawing process so as to explore the possibilities of reduction of number of stages required to manufacture a particular component.
Following are the conclusions drawn from the study.

- It has been found that by FEA analysis of deep drawing process, the present process of being carried out by industry that required four stages to manufacture can be done in three stages by combining the first two stages of process at room temperature condition.
- Simulating warm deep drawing process, using properties of material at elevated temperature that is 120° C, it has been found that first three stages of four stage process can be combined in one stage Therefore the total number of stages required to manufacture the component can be reduced to two, showing the approximate reduction in manufacturing time by about 35%.
- FEA results comparing room temperature deep drawing and actual experimental results of % of thinning of component at various points matches very well

showing that FEA simulation can be advantageously used for any product development.

- The prevention of the failure of product taking place at room temperature was found to be avoided with successful drawing at elevated temperature.

- It is found a reduction of approximately about 40% in load required while going for warm deep drawing.

- The effect of warm deep drawing on FLC is as follows.
  The FLD_o was found to shift downward from 0.34 to 0.28.

- Warm deep drawing has the potential to increase the productivity, It should be explored by industry.

8.2 Future Scope

- Effect of strain rate in conjunction with elevated temperature for warm deep drawing can be analyzed.

- The strain path can also be used as one of the parameter for determination of formability of metal under going warm deep drawing process.

References

[1] Metal Working, *Sheet Metal Forming*, ASM Handbook, Volume 14B, 2006, U.S.A.

[2] Surender Kumar,*Technology of metal forming process*,prentice-Hall of india private limited, page 2,37,73,(2008).

[3] B.L.Juneja,*Fundamentals of metal forming processes*,New age international publishers, page 108,317,381(2010).

bibitemDr. S .Singh Dr.Sadhu singh,*Theory of plasticity and metal forming process*Khanna publication, page 276,415(2006).

[4] S. Kurukuri, A. Miroux, M. Ghosh., *Effect of temperature on anisotropy in forming simulation of aluminium alloys.*, Journal of Material Processing Technology,Volume 161, page 178-186, (2004).

[5] ohannes Winklhofer, Gernot Trattnig, Christoph Lind. , *Process simulation of aluminium sheet metal deep drawing at elevated temperatures.*, Journalof material processing Technology,Volume 130-131, page 20-30,(2002).

[6] Hong Seok Kim, Muammer Koc Jun Ni. , *Development of an analytical model for warm deep drawing of aluminum alloys*, Journal of Material Processing Technology,Volume 197, page 393-407, (2008).

[7] F. Stachowicz, T. Trzepiecinski, *Warm forming of stainless steel sheet*, ARCHIVES OF CIVIL AND MECHANICAL ENGINEERING, Vol. X,page 111-1184, (2006).

[8] Jae Dong Lee, Young Moo Heo, Sung Ho Chang, *A Study on the Warm Deep Drawability of Sheets in Cr-Coated Die*, , KSME International Journal ,Vol. 15, page 839-846, (2001).

[9] Johhaness winklhofer, gernot tratting, Christoph Lind., *of aluminium sheet metal deepdrawing at elevated temperatures using LS-Dyna*, LSDYNA FORUM , bamberg 2010.

[10] G. Palumbo, D. Sorgente, L. Tricarico,S.H. Zhang,W.T. Zheng. *Effect of temperature on LDR is studied for material AZ31 using FEA analysis.*, KSME International Journal ,Vol. 19 , page 1139-1152, (2003).

[11] H. Takuda, K. Mori, T. Masachika, E. Yamazaki ,Y. Watanabe, *Finite element analysis of the formability of an austenitic stainless steel sheet in warm deep drawing*,Journal of Materials Processing Technology ,Vol. 143-144, page 242-248, (2003).

[12] ASTM Handbook, *Standard test methods and Definitions for Mechanical Testing of Sheet Product*, ASTM A370, (2011), U.S.A.

References